Chemical Science

ROYAL SOCIETY OF CHEMISTRY

REVIEW

View Article Online
View Journal | View Issue

Cite this: *Chem. Sci.*, 2024, **15**, 17781

When microplastics/plastics meet metal–organic frameworks: turning threats into opportunities

Pengfei Wu,†[a] Mengting Guo,†[a] Ran-Wei Zhang,[c] Qing Huang,*[abc] Guibin Wang*[a] and Ya-Qian Lan *[b]

Significant efforts have been devoted to removal and recycling of microplastics (MPs; <5 mm) to address the environmental crises caused by their ubiquitous presence and improper treatment. Metal–organic frameworks (MOFs) demonstrate compatibility with MPs/plastics through adsorption, degradation, or assembly with the MPs/plastic polymers. Above 90% of MPs/plastic particles can be adsorbed on MOF materials *via* the hydrophobic interaction, electrical attraction, π–π stacking, and van der Waals forces. Meanwhile, certain MOFs have successfully converted various types of plastics into high-valued small molecules through thermocatalysis and photocatalysis. In thermocatalysis, the primary process should be C–O bond cleavage, whereas in photocatalysis it ought to be the generation of reactive oxygen species (ROS). Moreover, the construction of novel MOFs using waste MPs/plastics as the ligands was mostly accomplished through three dominant ways, including glycolysis, hydrolysis and methanolysis. Once successfully composited, the MOF@plastic materials illustrated tremendous promise for interdisciplinary research in multifunctional applications, including sewage treatment, gas adsorption/separation, and the preparation of microbial fuel cells, plastic scintillators and other sensors. The review explicated the relationships between MPs/plastics and MOF materials, as well as the challenges and perspectives for their development. It can provide a deeper understanding of how MOFs remove/degrade MP/plastic particles, how MPs/plastics are recycled to prepare MOFs, and how to build multifunctional MOF@plastic composites. Overall, this analysis is anticipated to outline future prospects for turning the threats (MPs/plastics contamination) into opportunities (*e.g.*, as ligands to prepare MOF or MOF@plastic materials for further applications).

Received 4th August 2024
Accepted 1st October 2024

DOI: 10.1039/d4sc05205f

rsc.li/chemical-science

1. Introduction

The ever-growing usage of plastics creates serious environmental problems in earth systems.[1] Recent data reported that around 367 million tons of plastic were produced in 2020.[2] Considering the recent coronavirus (COVID-19) outbreak, extensive use of personal protective equipment will inevitably accelerate the trend, with an annual growth rate of about 10%.[3,4] After being used, approximately 79% recalcitrate in the environment and eventually fragment into microplastics (MP; ≤5 mm).[5,6] Individuals were thought to be inevitably exposed to MPs *via* ingestion and inhalation, leading to MP-related health hazards including oxidative stress, inflammation and even neurological dysfunctions.[1] MP exposure at the environmental levels (0.0125 mg mL^{-1}) has been linked to mitochondrial damage in both normal human hepatic and lung cells, resulting in overproduction of mitochondrial reactive oxygen species and inhibition of mitochondrial respiration.[7] Not only at the cell levels but MP accumulation in organs could induce gut microbiota dysbiosis (inflammatory responses)[8,9] and alter the biotics (*e.g.*, fishes and mice) movement and memory (neurological dysfunctions).[10,11] For example, MPs cause varying degrees of harm to adult grass shrimp with mortality ranging from 0% to 55%.[12] A latest study also found that exposure to MPs in mice altered the expression of neuronal genes and finally caused behavioural changes.[11] In addition, plasticizers released during the plastic waste fragmentation could also be transferred into the human body, disturbing the immune system and causing neurological dysfunctions *via* the absorption, distribution, metabolism, and excretion (ADME) processes.[13]

Given the upsurge in the generation of plastics and the severe ecotoxicity of MPs in the earth systems, pioneering scientists have begun to emphasize the importance of conceiving effective strategies to mitigate MP or plastic contamination.[14] The treatments for MPs could be generally

[a]*State Key Laboratory of Tree Genetics and Breeding, Co-Innovation Center for Sustainable Forestry in Southern China, Nanjing Forestry University, Nanjing, 210037, China. E-mail: huangqing@njfu.edu.cn; Guibinwang99@163.com*

[b]*School of Chemistry, South China Normal University, Guangzhou, 510006, China. E-mail: yqlan@m.scnu.edu.cn*

[c]*Co-Innovation Center of Efficient Processing and Utilization of Forest Resources, College of Materials Science and Engineering, Nanjing Forestry University, No. 159 Longpan Road, Nanjing 210037, China*

† These authors contributed equally to the work.

classified as traditional and circular economic solutions. Traditional treatments (*e.g.*, sedimentation and membrane filtration) temporally separate them from the hydrosphere but transfer them into the lithosphere through the sludge disposal,[15,16] during which a great challenge is how to isolate and collect them from environmental matrices.[17] Incineration and landfill are usually applied, but they cause energy dissipation and secondary pollutants (*e.g.*, dioxins). More and more attention has been paid to circular economic solutions, requiring plastic waste to be guided by the "3R" principles: reduce, reuse and recycle.

On the basis of the concept, three novel approaches to mitigate MP pollution are developed to transfer/degrade them into nontoxic or even highly-valued substances.[18–21] First, with the help of adsorption materials, large numbers of MPs could be concentrated and collected by advance materials for further treatments. For example, catalytic degradation (*e.g.,* electrocatalysis and photocatalysis) can be applied to cleave the polymer backbones by producing carbonyl groups, promoting the decomposition of plastics into high-valued products such as carbon nanotubes, hydrogens and hydrocarbons.[18,22–24] Second, plastic oligomers like terephthalic acid (TA) could be recycled and reused as raw materials, supplying effective organic linkers to build novel materials, especially metal–organic frameworks (MOFs), for further applications, including adsorption, catalysis, and so on.[25–28] Third, recent studies also take the benefits of the properties of MPs/plastics (*e.g.,* stable) and novel material (*e.g.,* tunable) to not only accomplish the reuse and recycling of MPs/plastics but also prepare economically functional materials with excellent physiochemical characteristics (*e.g.,* catalysis or sensing) for further applications.[26,29,30]

The key to implementing the three MPs/plastics treatment methods is to choose promising and readily available materials with high adsorption capacity, strong catalytic characteristics, or other multifunctional applications. MOF materials constituted by metal nodes and organic linkers are inevitable topics that attract broad interest in the reuse and recycling of MPs/plastics.[31,32] First, MOF materials with superior adsorption capacity and strong catalytic character can first converge MPs together and then fulfill the photo- and electro-catalysis processes for the conversion of MPs/plastics into high-valued products. C=O bonds have a greater bond-cleavage enthalpy of (799 kJ mol^{-1}), allowing for the development of MOFs that bypass the weaker C–C (347 kJ mol^{-1}) in the main chain or open the benzene branch (518 kJ mol^{-1}) of plastic polymers.[33] Second, several novel MOFs have been constructed from metal nodes and plastic-based organic linkers. Plastic polymers with one-third of the price of the same MOF linkers were provided by Sigma Aldrich or Basolite A100.[34] Plastic-based TA, ethylene glycol (EG), dimethylterephthalate (DMT), and bis(hydroxyethyl)terephthalate (BHET) obtained from PET bottles meet the requirements for preparing MOFs with low-cost, high-quality, and easy-recyclability. In addition to acting as the organic linkers, some plastics as ideal platforms facilitate the formation of MOF materials with complex structures (as the third aspect). The strategy could combine the benefits of two materials for the construction of MOF@plastic devices.[26,29,30] Therefore, it is of great necessity to realize the interactions between MPs/plastics and MOF materials, as well as the potential applications of MOF@plastic materials in increasing efficiencies of adsorption capacity, gas separation, catalytic properties, electrical transfer, scintillation, and sensing performance.[26,29,30]

Herein, we first introduced the current state of applying advanced MOF materials to adsorb and degrade MPs/plastics, including efficiency, selectivity, degraded products and underlying mechanisms. Afterwards, we summarized the creation of MOFs using plastics as the ligands or products/devices comprising MOFs and plastics of various types, as well as their mechanisms and applications. We finally discussed the assembling methods and value of novel MOF@plastic composites in various fields such as adsorption, catalysis and sensing.[29,35,36] By exploring the relationships between MPs/plastics and MOF materials (Fig. 1), this study will contribute to a deeper insight into the degradation and reuse of MPs/plastics, as well as help outline prospects for additional detection of potential MOF@plastic applications.

2. Literature retrieval methodology

For thoroughly locating the literature, multiple databases were searched with related phrases in titles, abstracts or keywords: Web of Science, Springer Link, ACS publication, Scopus and Google Scholar on July 2nd, 2024. English references in the latest 10 years were summarized prior to being selected for

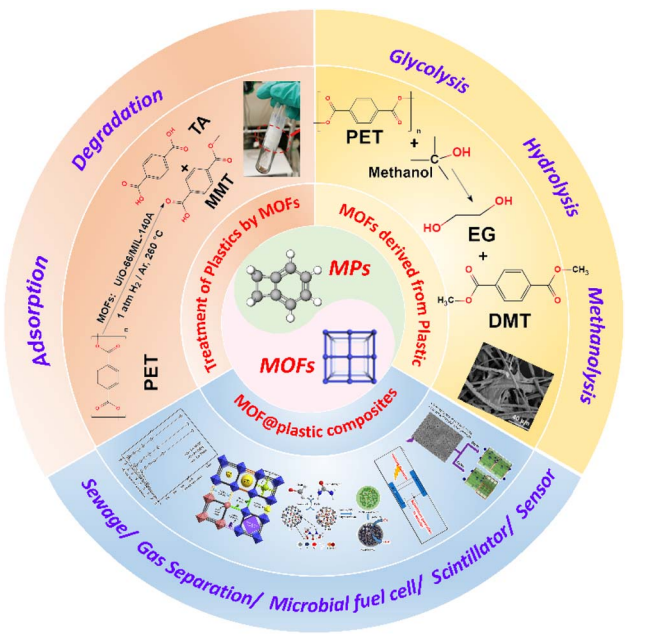

Fig. 1 Relationships between MPs and MOFs, including the current state of applying advanced MOF materials to adsorb and degrade MPs/plastics, the preparation of MOFs using plastics as the ligands or products/devices comprising MOFs and plastics of various types, and the multifunctional applications of novel MOF@plastic composites in various fields. The study will contribute to a deeper insight into the degradation and reuse of MPs/plastics, as well as help outline prospects for additional detection of potential MOF@plastic applications.

Table 1 Applications of MOFs or plastic-based MOFs for adsorption or degradation of MPs, NPs, and other contaminants

MOF or MOF@plastic composites			Target substances			Conditions					
Name	Character	Efficiency	Name	Composition	Size (nm)	pH	Temp. (K)	Conc. (ppm)	Mechanism	Advantages	Ref.
Adsorption											
ZIF-67	30–600 nm	92.1%	MPs	PS	1000–3000	3–12	288–308	0.005	H bonding, π–π and electrostatic interactions	High efficiency; short time; simple operation	123
MIL-101 (Cr)	2.91 nm (~0.23 cm^3 g^{-1})	96%	NPs	PS	65	5–10	298	5–100	Electrostatic, π–π interaction	High efficiency; high stability	124
UIO-66-X (X = H, NH_2, OH, Br, NO_2)	100–200 nm; 0.022–0.34 cm^3 g^{-1}	85.7–95.5%	NPs	PS, PMMA, and PVDF	183–325	—	—	0.5–2	H bonding; electrostatic and van der Waals interaction	Abundant sites; high stability; high affinity	125
ZIF-8	2–3 μm	91.4%	NPs	PS, PVDF	90–140 (PS) 60–110 (PVDF)	—	—	0.5	Electrostatic and hydrophobic interaction; H bonding	Good efficiency; wide feasibility	40
PSF*/MIL-100 (Fe)	~3.5–8 nm	99%	MPs	PE and PVC	4.25×10^4 (PE) 1.34×10^5 (PVC)	3–11	—	10–100	—	High rejection; high flux; high stability	126
Nano ZIF-8 (Fe)	500–1100 nm	98%	MPs	PS	1100	—	—	25	Hydrophobic interaction, H bonding	Abundant sites; high efficiency; high stability	39
MOF@C@FeO	749.7 m^2 g^{-1}	~100%	MPs	PS	1000	2.5–12.5	40–60 °C	200–1000	Hydrophobic, π–π, and electrostatic interaction	High stability; high efficiency	41
UiO-66(NH_2/OH)	433–1015 m^2 g^{-1}	~100%	NPs	PS	26	—	—	20–1000	Electrostatic interaction	Cost-effectiveness	43
PET-based UiO-66(Zr)	1139.2–1603.25 m^2 g^{-1}	~35%	Ketorolac tromethamine	Drug	—	2–10	308	10–100	Electrostatic interaction	Economic; high stability	73
PET-based MOF (Cu)	9–24 μm	90–96%	Methylene blue	Dye	—	2–8	288–313	2–200	Electrostatic interaction; physical adsorption	Economic high stability	74
PET-based MOF (Fe-, Zr-, La-)	128.3(Fe) 290.4(Zr) 61.8(La)	(70.02–114.28 mg g^{-1})	As	Heavy metals	—	7	—	100	H bonding, π–π stacking, electrostatic interactions	Economic; high stability	30
ZIF-8@plastic	234 m^2 g^{-1}; 0.205 m^3 g^{-1}; 730–850 nm	95.8–99.5%	$PM_{2.5}$; PM_{10}	Fine particles	—	—	353–573	0.2 m S^{-1}	—	High stability	46
Gas storage											
PET-based MOF (Cr)	2618–3233 m^2 g^{-1}	1.8–2.1% (wt)	H_2	Gas	—	—	—	—	Large specific surface area	Economic	79

Table 1 (*Contd.*)

MOF or MOF@plastic composites			Target substances			Conditions					
Name	Character	Efficiency	Name	Composition	Size (nm)	pH	Temp. (K)	Conc. (ppm)	Mechanism	Advantages	Ref.
PET-based MOF (Zr)	602–948 m^2 g^{-1}	1.38% (wt)	H_2	Gas	—	—	—	—	Large specific surface area	Economic	80
Name	**Character**	**Yield efficiency**	**Name**	**Type**	**Character**		**Temp.**	**Weight**	**Products**	**Advantage**	
Degradation											
UiO-66 (Zr)	600–1160 m^2 g^{-1}; 24–67 nm; 9.2 mg	16–98%	MPs	PET	Fragments	—	493	21.3 mg	MMT + TA; β-scission process	High efficiency; waste-to-resource	45
MOF (Ln)	523–564 m^2 g^{-1}; 138.6 mg	24.6–50%	Plastic	poly(g-butyrolactone)	Fragments	—	433	48.0 mg	γ-Butyrolactone	—	47
Ag_2O/Fe-MOF	110–1402 m^2 g^{-1}; 2–20 nm; 0.1 g	—	MPs	PET, PE, and PEG	Microbeads, bulks	—	298	0.5 g	Acetic acid, ethanol, formic acid, H_2	Waste-to-resource	48

further examination. A detailed review was conducted on the research areas of "chemistry/biochemistry/electrochemistry", "materials science", "environment science", "physics" "polymer science" and "engineering/instrumentation". The inclusion criteria in the next paragraph were established for "publication years", "language", and "research area".

A comprehensive search was undertaken using the keywords "polymer", "plastic", "microplastics", "nanoplastics" and "metal–organic frameworks". About 104 articles are related to MPs or plastics and MOFs from 1993–2023. There are 14, 39, and 98 articles, respectively in the ISI Web of Science database that analyze the degradation of MPs/plastics by MOFs, the recycling of MPs/plastics to prepare MOFs, and the generation of MOF@plastic composites (with the phrases of MPs/plastics + MOFs + degradation, MPs/plastic + MOFs + recycle/reuse, and polymer + MOFs). After screening the inclusion criteria, 95 publications were manually chosen by reviewing titles, abstracts, and entire content in cases of uncertainty. In addition, valuable information (*e.g.,* books and reports) was also provided to summarize the relationships between MPs/plastics and MOF materials.

3. Adsorption of MPs/plastic particles by MOF materials

MPs or plastics as contaminants can result in various detrimental effects on the aquatic ecosystems, including oxidative stress, inflammation, and immunological/neurological dysfunctions.[13] The ecotoxic effects might be magnified due to biomagnification and bioaccumulation. The removal of MPs/plastics from aquatic ecosystems has received increased attention in recent studies (Table 1).[37] Adsorption with its versatility and cost-effectiveness has been regarded as one of the most effective techniques.[38] Because MOFs have a large specific surface area (SSA) and high porosity, many publications have reported their distinguished adsorption capacity for MPs.[39–41] A research study utilizing ZIF-8 MOF demonstrated a 98% removal efficiency of PS MPs at high concentrations (25 mg L^{-1}) within 5 min coagulation (Fig. 2a).[39] Taking advantage of magnetic adsorbents, MP-attached ZIF-8 MOFs achieved rapid separation in a few seconds from Milli-Q water, residential and laboratory tap water environments (Fig. 2b). Another study identified a two-dimensional MOF nanopillared structure (2D MOF@C@FeO) as a promising adsorbent for MP removal.[41] The 2D MOF@C@FeO displayed a large SSA (749.7 m^2 g^{-1}), abundant active stress, and magnetic properties. It successfully eliminated MPs by ~100% within the first hour of contact. After six cycles, the reusability of 2D MOF@C@FeO remains at 90% removal capacity (Fig. 2c). These studies clearly demonstrated that MOF materials have considerable promise for sorbing and eliminating MPs from aquatics. However, these studies on MP removal by MOF materials are still in the early stages. The adsorption settings are simplistic, using Milli-Q water or the simulated tap water. Strengthening adsorption research is necessary, particularly in terms of expanding adsorption

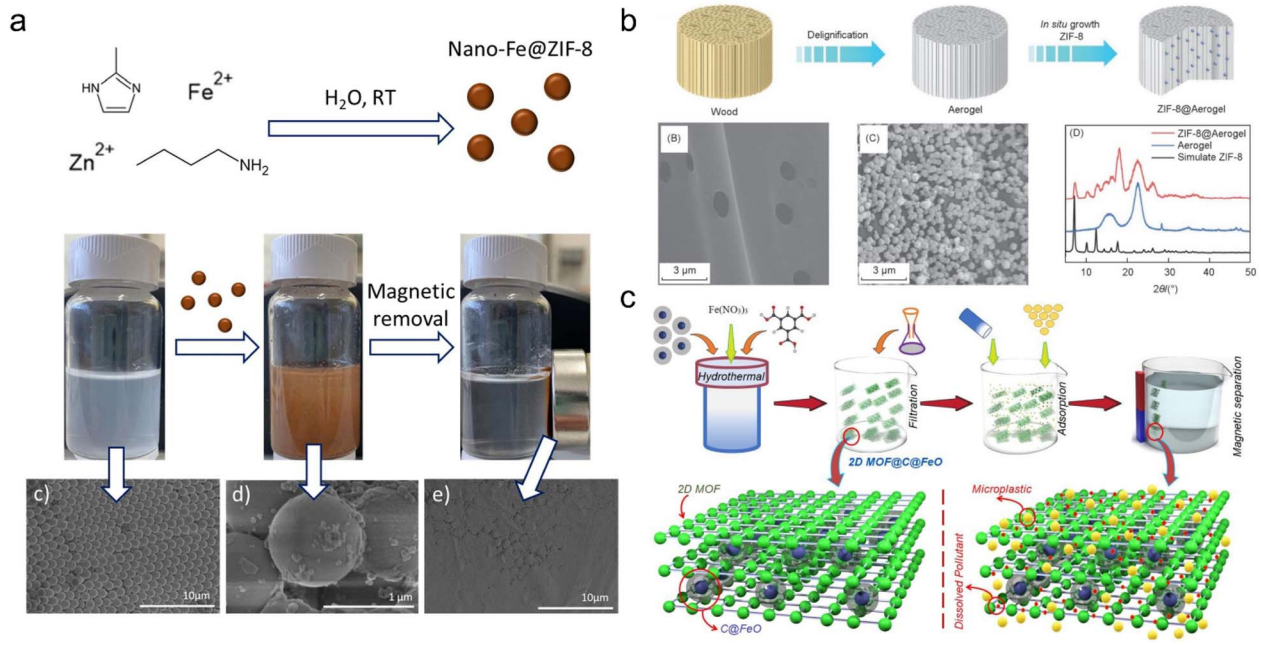

Fig. 2 Adsorption of MPs/plastic particles by MOF materials. (a) ZIF-8 MOF adsorbed MPs with high removal efficiency (98%) and rapid adsorption rate (within 5 min). This figure has been reproduced from ref. 39 with permission from Elsevier Science, copyright 2022; (b) A ZIF-8@Aerogel MOF material was developed for effective adsorption of micro- and nano-plastics (removal efficiency of 85.8% for polystyrene and 91.4% for poly(1,1-difluoroethylene)). This figure has been reproduced from ref. 40 with permission from Springer Nature, copyright 2022; (c) another carbon-based MOF materials exhibited good reusability with MP removal efficiency remaining at 90% after six cycles. This figure has been reproduced from ref. 41 with permission from Elsevier Science, copyright 2023.

habitats, and studying adsorption kinetics, isotherms and thermodynamics.

According to the previous studies, some possible mechanisms of the interaction can be determined from the physiochemical features of MPs and MOFs. First, the comparably high hydrophobicity of MPs and MOFs indicated that hydrophobic interaction could easily attract and deposit MPs on MOF surfaces.[39–41] Second, MPs in aqueous medium frequently have negative τ-potentials and offer good affinities with positively charged MOFs, such as the 2D MOF@C@FeO and nano-Fe@ZIF-8.[39–41] Some MP functionalized groups could also affect the interaction.[42,43] The presence of benzene rings indicates that π–π stacking could accelerate the removal of PS MPs.[41] Numerous $-CF_2-$ units on polyvinylidene fluoride (PVDF) MPs formed hydrogen bonding in aqueous medium, thereby enhancing the adsorption efficiency of PVDF on MOFs (*e.g.*, the hydrogen bond energy for OH–F is 2.4 kJ mol^{-1}).[44] According to these fundamental principles, several parameters influencing MP adsorption capability on MOFs could be theorized, including pH, temperature, MOF structure and the existence of dissolved or natural organic matter (NOM). However, there is a lack of experimental evidence regarding the aforementioned concerns. Future knowledge on the interaction between MPs and MOFs should focus on gaining more interaction mechanisms (*e.g.* π–π stacking and hydrogen bonds) or environmental interference (*e.g.* pH and NOM).[42,43]

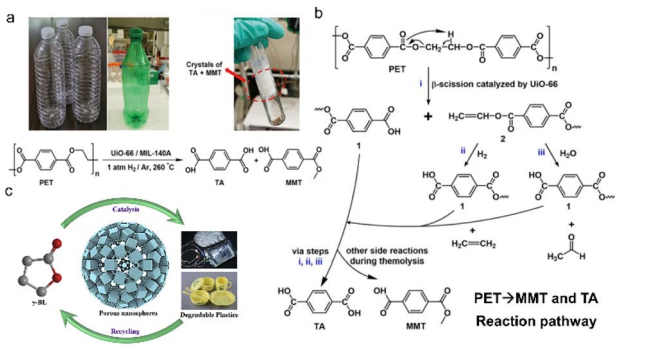

Fig. 3 Catalytic degradation of MPs/plastics by MOF materials. (a) Terephthalic acid (TA) and mono-methyl terephthalate (MMT) were successfully derived from plastic bottles under the catalysis of zirconium (Zr)-based MOF, with the max yield of the TA and MMT reaching 72% and 30% in 1 atm H_2 condition (24 h at 260 °C); (b) recycling degradable plastics for γ-butyrolactone production, which was further applied for preparation of lanthanum-based MOF catalysts with the strategy conducted at 220 °C for 1 h; (c) proposed reaction pathway for the degradation of PET catalyzed by UiO-66. This figure has been reproduced from ref. 45 with permission from John Wiley and Sons, copyright 2022.

4. Catalytic degradation of MPs/plastics by MOF materials

Various MOF materials can convert MPs/plastics of one or more types into a mixture of hydrocarbons, hydrogen, carbon nanotubes, carbon monoxide and liquid fuels (Table 1).[18,22] MMT and

TA were successfully derived from plastic bottles, mostly PET, under the catalysis of zirconium (Zr)-based MOF. Within 24 h at 260 °C, the maximum yield of the MMT and TA could reach 30% and 72% in 1 atm H_2 conditions, respectively (Fig. 3a).[45] TA is a raw material that could be used to reproduce PET or as the linker in the synthesis of other MOF materials.[46] The work served as a guide for MPs/plastic degradation by MOF catalysts in the recycling economy. Another lanthanum (Ln)-based MOF material with a large specific surface area (823 $m^2\ g^{-1}$) and tremendous active sites has been designed to generate γ-butyrolactone (~100%) from poly(γ-butyrolactone) plastic.[47] γ-butyrolactone has long been used as a paint stripper, superglue remover, and stain remover (Fig. 3b). Despite the extensive applicability of MOF catalysts, the strategy still required a heat treatment at 220 °C for 1 h, potentially consuming heat energy. Therefore, seeking accessible energy saving conditions has sparked widespread interest.

To decrease energy consumption, many other researchers have attempted to utilize solar-driven photocatalysis to convert MPs along with the generation of hydrogen (H_2).[48,49] A series of novel catalysts containing both light absorption and electron transport capacities were synthesized. For instance, Ag_2O/Fe-MOF photocatalysts were fabricated exhibiting a wide solar light-harvesting range and could enable the generation of H_2 and value-added chemicals, including formic acid, ethanol and acetic acid.[48] In their work, 0.2 wt% of Ag_2O/Fe-MOF photocatalyst transformed 27.5 mg (~6.4×10^9 items) of polyethylene glycol (PEG) MPs. In light of these findings, 32 unactivated alcohols could be obtained from a variety of hydroxyl-terminated polymers (*e.g.,* PEG, polycaprolactone) and even non-biodegradable PE plastics.[49] These studies provided fresh insights into developing unique MOF photocatalysts to address the global plastic waste crisis along with implementing renewable high-valued materials.

On the basis of the strategies documenting the conversion of MPs/plastics into value-added chemicals, the catalytic mechanisms are diverse and need to be revealed. Under thermolysis conditions, Zr-MOFs first catalyze and hydrolyze the C–O bonds in ester groups, yielding vinyl-terminated carboxylate and carboxylic acid-terminated units. The vinyl-terminated carboxylate would then undergo hydrogenolysis with H_2, forming numerous carboxylic acid-terminated units (Fig. 3c). Following the continuous thermolysis, MMT and TA should finally be formed after the fraction of vinyl-terminated carboxylate units,[45] and the thermo-processes provide the main energy during the entire hydrogenolysis. During photocatalysis, MOF materials could harvest the light and produce reactive oxygen species (ROS), such as superoxide and hydroxyl species.[50] ROS could activate MPs/plastics by shedding hydrogen to generate R· (activated MPs/plastics molecules). The R· further reacted with oxygen to produce ROO·, which could then divest hydrogen to generate hydroperoxides (ROOH). ROOH could afterwards generate ROO· and ·OH groups through chain propagation reactions. ROS in photocatalysis is formed not only by the interaction of photo-activated MPs and oxygen but also by the interaction of electrons or holes from the photocatalyst with oxygen adsorbed on its surface. For example, electrons move from Ag_2O to the conduction band of Fe-MOF catalysts,

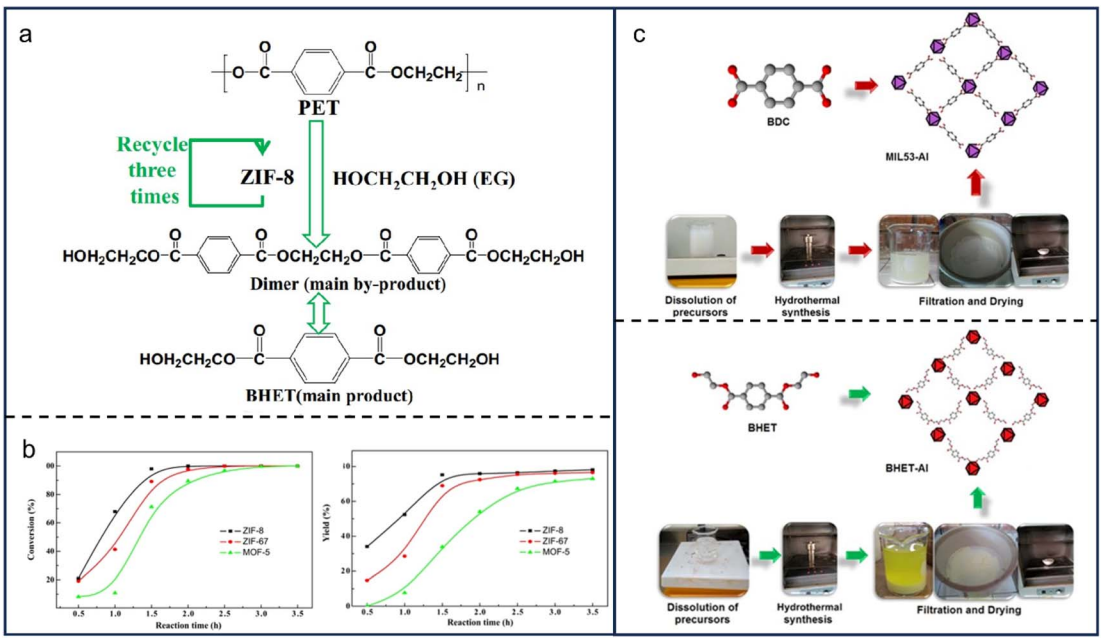

Fig. 4 Synthesis of MOF materials from MPs/plastics. (a) Production of bis(hydroxyethyl)terephthalate (BHET), ethylene glycol (EG), and other oligomers through glycolysis; (b) a series of MOFs, including MAF-6, ZIF-8, ZIF-67, and MOF-5 were successfully prepared from BHET and various metal ions at nearly 100–200 °C for several hours. The figures (a) and (b) have been reproduced from ref. 56 with permission from Springer Nature, copyright 2017; (c) synthesis procedure of MIL53-Al and BHET-Al MOFs. This figure has been reproduced from ref. 54 with permission from Springer Nature, copyright 2021.

participating in generating $\cdot O_2^-$ and H_2. Simultaneously, the holes on the valence band of Fe-MOF were transferred to that of Ag_2O, resulting in the formation of $\cdot OH$. Finally, the produced ROS were employed to decompose the MPs/plastics into short-chain organic molecules.[48] Due to the related studies still in their infancy, the cascade photocatalysis of MPs/plastics remains unclear, and the corresponding intermediates are diverse. Thus, more efforts are being made to understand the path and mechanism of the photocatalytic conversion of plastics.

5. Synthesis of MOF materials from MPs/plastics

Plastics with high durability, strength and cost-effectiveness have been extensively utilized in daily lives.[6,13] However, only 9% have been recycled, indicating a high recycling demand. Since plastics could produce organic linkers for MOF materials (*e.g.,* TA depolymerized from PET), recent studies have focused on the subject and then been summarized as glycolysis, hydrolysis and methanolysis.[51,52]

5.1 Glycolysis

Glycolysis is the transesterification of EG and PET ester groups. Typically, it is performed under catalysis of sodium carbonate, zinc acetate, cobalt acetate, and lead acetate. The products contain EG, BHET, and other oligomers (Fig. 4a). EG as a solvent in the reactants is also produced during the process, demonstrating that the reaction rate of glycolysis is not affected by reactants' concentration but by some other issues like polymer surface area.[53] The reaction would be more effective if the particles were smaller or mixed more vigorously. BHET also acts as a precursor in the synthesis of MOFs. For instance, Cabrera-Munguia *et al.* reported the synthesis of a highly crystalline MOF named BHET-Al from BHET and aluminum nitrate.[54] Heating at 200 °C for 72 h produced a material with high thermal stability, a macroporous structure, and excellent gas adsorption properties. Similarly, a series of MOFs, including MAF-6, ZIF-8, ZIF-67, and MOF-5, were successfully synthesized from BHET and various metal ions at nearly 100–200 °C for several hours (Fig. 4b and c).[55,56] In addition to EG and BHET, additional monomers derived from plastic glycolysis, such as dimethyl terephthalate and dimethyl isophthalate, could be used for MOF synthesis.[57]

Glycolysis has various advantages, including cost-effectiveness, mild reaction conditions, high quality and purity, and tunable properties. First, glycols are readily available, inexpensive, and non-toxic, making them highly appealing from both an economic and environmental standpoint.[57] Second, the mild circumstances for a glycolysis reaction to happen.[58] A temperature of 120–150 °C is demanded, much lower than that of traditional MOF synthesis. Third, the progressive release of metal ions allows for better control over crystal nucleation and growth. Last but not least, glycol modification can straightforwardly change the surface area, pore size, and chemical functionality of MOFs, providing a high degree of tunability and flexibility.[59] However, it's worth noting that one significant disadvantage of glycolysis is the difficulty in separating the resultant oligomers from the products. The challenge may limit the purity and scalability of MOF production.[60]

5.2 Hydrolysis

Hydrolysis is a chemical reaction that uses water to break down the lengthy chains of polymer molecules that comprise the plastic into smaller molecules.[61] It is often conducted in strong acid/base solutions at high temperatures and pressures, with catalysts to speed up the reaction (Fig. 5a). The choice of acidic or basic environments usually depends on the nature of the MPs and expected products. The acid reacts with the MPs, converting the polymer chains into smaller molecules, such as carboxylic acids, alcohols, and aldehydes. The molecules can coordinate with metal ions, act as bridging ligands for metal nodes, and finally form MOFs with high porosity, huge SSA, and adjustable topologies. In strong basic circumstances, bases could also attack the ester linkages to form EG and monosodium/disodium terephthalate salt (DST). DST could help restore the monomer TA in acidic situations. Once the hydrolysis event occurs, the generated small molecules serve as organic linkers to cooperate with the metal ions. Other conditions like high temperature, high pressure and the presence of catalysts aim to accelerate and improve hydrolysis efficiency. Recent publications have widely reported on the use of hydrolysis to degrade MPs into organic linkers (Fig. 5b).[62–64] Yang *et al.* used TA (0.1 g mL^{-1}) as an acid catalyst to promote PET hydrolysis at 220 °C for 180 min. The results revealed that the conversion rate of PET achieved almost 100%, while TA yield was up to 95.5% with a high purity of 99%.[62] Although the technology used in acidic settings necessitates higher temperatures and longer time, the products' yield and purity, and the stability of catalysts, indicate considerable potential for industrialization. Alkaline hydrolysis

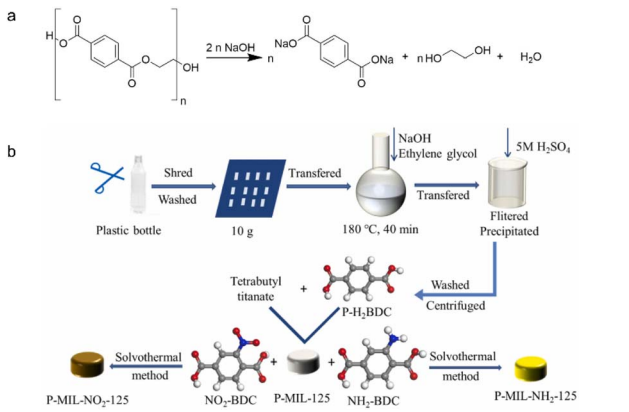

Fig. 5 Small molecules generated from the fragmentation of plastics through hydrolysis. (a) Scheme of the generation of carboxylic acids, alcohols, and aldehydes in strong base solutions. This figure has been reproduced from ref. 60 with permission from De Gruyter, copyright 2021. (b) Scheme of the generation of organic linkers (P-H_2BDC, NH_2-BDC, NO_2-BDC) through hydrolysis. This figure has been reproduced from ref. 63 with permission from Elsevier Science, copyright 2022.

resulted in the complete disintegration of TA and EG at 60–90 °C after 3 h, both of which are building blocks for MOF materials. The study described industrial prospects for hydrolyzing additional polymers with water-sensitive groups (*e.g.,* polyamides, polyethers, and polycarbonates).[64]

Hydrolysis, like glycolysis, has high efficiency and purity, as well as environmental benefits. Moreover, it offers several other advantages, like recyclability, and ease of product separation. For example, Yang *et al.* observed that TA yield could be maintained at 93.3–95.6% after 8 cycles.[62] Meanwhile, the high purity of 99% suggested high separation efficiency.[62] However, some complications associated with MP hydrolysis were also detected: First, hydrolysis is energy-intensive requiring high temperatures and pressures to achieve the desired condition.[65] Second, using strong acids or bases in the hydrolysis process can be corrosive, posing potential safety issues.[65] Third, although hydrolysis has shown promise for industrial applications, it still needs a long way to go because recent technologies may not be effective for all types of MPs, especially those that are resistant to hydrolysis.[66]

5.3 Methanolysis

Methanolysis is the conversion of plastics into methanol and other valuable products. The process involves the fragmentation of long polymer chains into smaller molecules using methanol as a solvent at high temperatures and pressures (Fig. 6a). The resultant product can be processed further to yield methanol and monomers, which can be used as a chemical feedstock (methanol) and raw materials for MOF production.[67,68] The major components of PET plastics under methanolysis were dimethylterephthalate (DMT) and EG, which are usually catalyzed by sodium carbonate or zinc acetate. Except for that, this transesterification to PET recycling suffers from the formation of a mixture of glycols, alcohols, and phthalic acid derivatives (Fig. 6b).[60] As DMT could be further broken down into TA and methanols, efforts should be made to isolate and purify DMT throughout this process.

Many benefits of methanolysis were found in converting plastics into high-valued chemicals. First, it contributes to reducing the large volume of plastic waste that ends up in landfills. Second, methanol is a renewable resource that is less harmful to the environment than other solvents used in chemical processes. Third, compared to other plastic conversions (*e.g.,* incineration or pyrolysis), the process emits fewer greenhouse gases and less toxic waste. The primary disadvantage of methanolysis is that the reaction must be carried out at high temperatures and pressures, which reduces the economic viability of upcycling PET polymers into highly-valued chemicals. Because the byproducts produced throughout the process are too excessive, the time required for the separation/purification of target products is another challenge.

6. Functional applications of MOF@plastic composites

When plastics are used as the basis material for MOFs, the polymers provide an ideal medium for incorporating MOFs into/onto structures.[69] MOFs feature abundant holes ranging from microscale to macroscale, which may accommodate a variety of species and provide effective adsorption or separation on MOF@plastic composites. Moreover, the introduction of MOFs with electrical, catalytic, and optical capabilities to the polymer-derived organic linkers is sufficient to develop the functionality of MOF@plastic composites.[28,35,70–72]

6.1 Sewage treatment

The presence of various contaminants in wastewater is a growing environmental concern that has detrimental impacts on human health.[13] The most common contaminants in wastewater include dyes, heavy metals and other pollutants. As

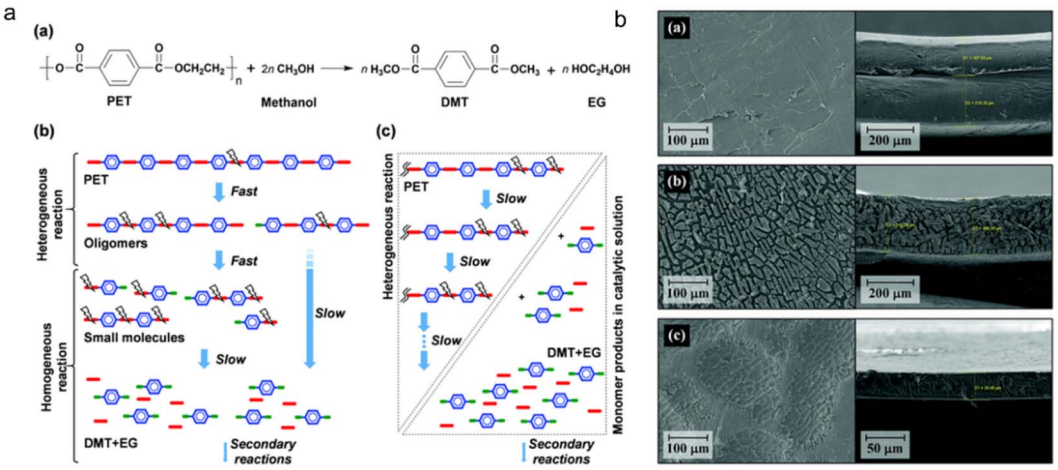

Fig. 6 Small molecules obtained using methanol as a solvent at high temperatures and pressures. (a) Major reaction step for PET depolymerization *via* methanolysis; (b) SEM images of the polymer surface (left) and cross-sections (right) after methanolysis of double-layered waste PET for 0 hour, 12 hours and 24 hours at 25 °C. The figures (a) and (b) have been reproduced from ref. 67 with permission from the Royal Society of Chemistry, copyright 2021.

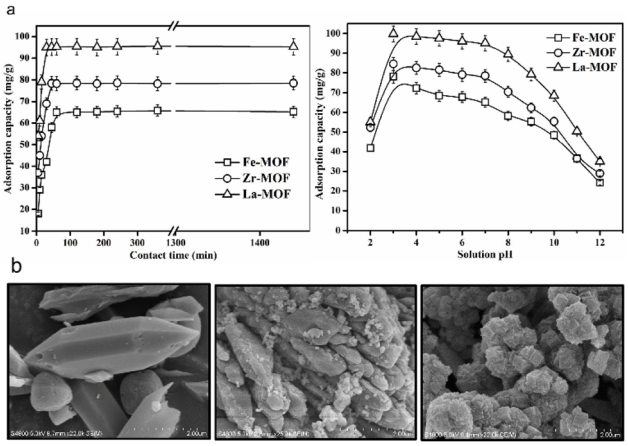

Fig. 7 Contaminant removal of plastic-based MOF composites (a) Adsorption of As by Fe-, Zr- and Ln-based MOF@plastic composites using a TA linker derived from PET bottle with high capacities of 70.02, 85.72, and 114.28 mg g^{-1}, respectively; (b) from left to right, are SEM images of metal–organic framework (MOF) for Fe-MOF, Zr-MOF, and La-MOF. The figure has been reproduced from ref. 30 with permission from Elsevier Science, copyright 2022.

mentioned, MOF@plastic composites have exceptional sorption abilities, and their use as adsorbents for the removal of contaminants in water treatment has been widely reported. For example, Kalimuthu *et al.* reported an approach for synthesizing Fe-, Zr- and Ln-based MOF materials using a TA linker derived from PET bottles, and further employed as an efficient adsorbent for arsenate (As) removal (Fig. 7a).[30] The three MOF@plastic materials were added in 20 mL of various As concentrations (40–140 mg L^{-1}). The adsorption processes achieved equilibrium within 120 min, with the maximal capacity of 70.02 (Fe-MOF), 85.72 (Zr-MOF), and 114.28 (La-MOF) mg g^{-1} (Fig. 7b). The adsorption of As onto the three MOF@plastic materials well followed the Langmuir isotherm and described by the pseudo-second-order model. The recyclability of the adsorbent found that the adsorption efficiency was reduced by <10% after four continuous adsorption/desorption cycles. Similar to heavy metals, a waste-to-resource approach for UiO-66 (Zr) MOF was established to examine its potential to remove pharmaceutical compounds, namely ketorolac tromethamine (KTC), from wastewater.[73] The highest adsorption of UiO-66 (Zr) MOF achieved 729.92 mg g^{-1} at around 120 min, with the same adsorption behaviours (kinetics: pseudo-second-order kinetics; isotherms: Langmuir model). After six cycles, the adsorption capacity of UiO-66 (Zr) remained at 515 mg g^{-1}, indicating its excellent recyclability. In contrast to As and KTC, a Cu-based MOF removed methylene blue (MB), a hazardous cationic dye, in wastewater solutions with different sorption behaviors.[74] The modelling predicted the Langmuir isotherm but the pseudo-first-order model suits better the adsorption process. After 20 min reaching equilibrium, the adsorption capacity achieved 41.01 mg g^{-1}, whereas reusability fell to 22.15 mg g^{-1}. These findings suggest that recycled plastic-derived MOF materials have outstanding adsorption properties and can be anticipated as a suitable candidate towards various contaminated water. However, the competitive adsorption and selectivity of MOF@plastic materials have not been studied. Therefore, the interference of other ions, chemicals and substances should be considered when determining the actual adsorption capacity of MOF materials in wastewater, and further research is required.

For the adsorption mechanisms, the difference in kinetics between As(v) and MB indicated that it might be driven by different forces. As(v) adsorption over PET-derived MOFs followed pseudo-second-order kinetics, suggesting chemical interactions of As–OH, As–O bonds forming between metal clusters and As Anions. In contrast, the adsorption of MB fitted better by the pseudo-first-order model, indicating that the physical interaction occurred *via* electrostatic attraction between negatively charged MOF@plastic materials and MB cations.[74] Because of the homogeneous surface of adsorbents, Langmuir models could better describe the adsorption processes of MOF@plastic materials. In this application, plastic-derived MOFs offer various advantages. First, MOF@plastic composites are generally constructed of porous carbon materials with diverse compositions and functionalities for efficient adsorption of specific contaminants. Second, composites derived from plastics are low-cost and easy to use for adsorption and subsequent separation during pollutant removal. Last but not least, reusing plastic waste as precursors for MOFs could promote sustainable waste management. Therefore, it is a promising field for developing MOF@plastic composites in order to establish a circular economic model.

6.2 Gas adsorption/separation

Gas purification is an essential process for producing chemical commodities used in industry. Specifically for the oil industry, it contributes significantly to annual earnings in the trillions of US dollars.[35] Gas adsorption/separation, defined as the process of selectively adsorbing/separating target gases from mixed gases to achieve the necessary purity, is crucial during gas purification.[75] Traditional separation relies on thermally driven technologies that involve multiple evaporation and condensation cycles. Advanced techniques such as adsorptive separation could save more than 10 times as much energy.[76] MOFs exhibit superior adsorption capacity and are gaining popularity for use in gas separation (Fig. 8a and b).

MOF@plastic composites have been extensively studied for gas adsorption. Dyosiba *et al.* employed PET bottles as a TA linker source to synthesize UiO-66 (Zr) and MIL-101 (Cr).[77–79] They prepared colorless and colored PET bottles as raw materials for TA production to synthesis UiO-66 (Zr). As a result, colorless and colored MOF@plastics composites exhibited similar results in SSA with the result of 814 m^2 g^{-1} for colorless and 933–1085 m^2 g^{-1} for colored UiO-66 (Zr), respectively. With such a high SSA, the H_2 storage capacities reached 1.5–2.1 wt%, which is comparable to or even higher than the commercial-derived MOF materials (1.8 wt%).[80] The successful economic MOFs encouraged more studies on the gas storage application of plastic-derived MOFs. Except for high H_2 storage (1.4 wt%), MIL-101 (Cr; SSA: 1022 m^2 g^{-1}) exhibited good capacities for

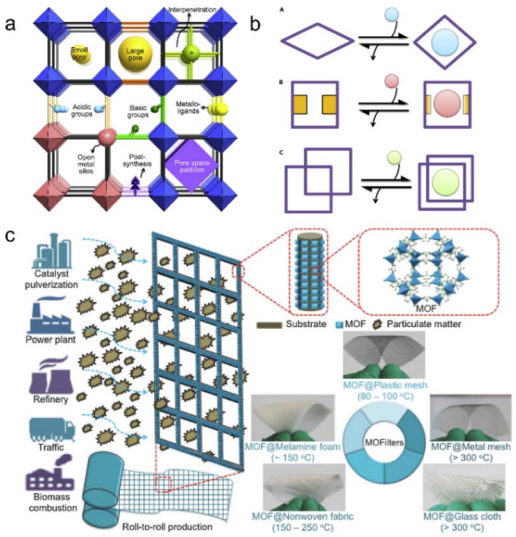

Fig. 8 Gas adsorption/separation by plastic-based MOF materials. (a) Microporous metal–organic framework materials for gas separation; (b) adjustable MOFs for separating and selecting different gases. The figures (a) and (b) have been reproduced from ref. 35 with permission from Elsevier Science, copyright 2020; (c) cheap plastic-based substrates such as screens, cloth, non-woven fabrics and melamine foam are used to produce MOF filters. The figure has been reproduced from ref. 47 with permission from John Wiley and Sons, copyright 2021.

CO_2 adsorption with 4.88 mmol g^{-1} at 293 K and 1 atm. Moreover, a series of low-cost plastic substrates (*e.g.*, mesh, cloth, nonwoven fabric, and melamine foam) were developed for the manufacturing of MOF filters and successfully applied to adsorb particulate matter (PM) from the atmosphere (Fig. 8c).[46] For example, all of them had substantial adsorption capabilities ($PM_{2.5}$: 99.5% and PM_{10}: 99.3% by ZIF-8@melamine foam at room temperature; $PM_{2.5}$: 96.8% and PM_{10}: 95.8% by ZIF-8@cloth at 200 °C). Notably, the adsorption capacity of ZIF-8@mesh was retained above 90% for 30 consecutive days, and its efficiency remained high after at least 3 simple cleans. These studies presented promising examples of a cost-effectively synthesized adsorbent for gas adsorption, which provides promising candidates for further gas separation.

Gas separation is the process of separating gas mixtures into their components. By finely tweaking pore size and immobilizing functional sites on the pore surface, MOF@plastic composites can be used for gas separations with high separation selectivity and productivity.[35] Zhou *et al.* designed a waste PET-derived hcp UiO-66(Zr) to selectively separate a mixed vapor of benzene/cyclohexane mixture, which other distillation methods cannot success because of the very close boiling points.[81] An equimolar benzene/cyclohexane vapor mixture (1 : 1) was injected into the column for separation. Hcp UiO-66(Zr) initially adsorbed both gases and then cyclohexane began to elute far before benzene, suggesting a good separation between the two compounds. When the saturation point was achieved, competitive adsorption of benzene/cyclohexane could be observed, and the findings demonstrated that the adsorption capacities of benzene and cyclohexane were estimated as 4.96 mmol g^{-1} and 2.19 mmol g^{-1}, respectively. The higher selectivity for benzene on hcp UiO-66(Zr) might be attributed to its similar structure to fcu UiO-66(Zr), where the adsorption of stacked benzene molecules by MOF pore walls occurred *via* the framework's tetrahedral cages. Despite having lower selectivity than previously reported commercial MOF materials (*e.g.*, DAT-MOF-1 and MOF-74), it provided a viable waste-to-resource scheme for reproducing MOF materials to separate industrial gas substances. Other gas mixtures, however, have yet to be separated by plastic-derived MOFs. Therefore, additional fundamental knowledge on the formation of MOF@plastic composites, together with the separation principle and efficiency, is required.

6.3 Microbial fuel cells

Microbial fuel cells (MFCs) are a promising solution to sustainable energy generation, leveraging the capabilities of microbes to convert organic matter into electricity.[82] MFCs have two chambers: aerobic (cathode) and anaerobic (anode). The cathode is mostly composed of conductive materials, whereas the anodic chamber responds by producing electrons and protons (*e.g.*, oxidized organic compounds). The electrons generated at the anode migrate through the external circuit to the cathode. At the same time, protons transfer from the anode to the cathode chamber.[83] Therefore, the fabrication of cathodes for MFCs is of great importance in attaining high power density and electricity.[26] However, the fact that the majority of polymers are electric insulators, with only a few examples of conducting polymers, presents a significant barrier to direct usage as nodes.[84] Many efforts have been made to prepare MFC by polymer-based MOFs as sustainable anode or cathode, which can be introduced for catalytic application in air cathode.[85] MOF materials may supply superior electrical catalytic oxidation–reduction reactions as an alternative to commercial Pt/C cathodes.[86] Plastics have been certified as effective organic linkers to MOFs, and numerous developments have been made on their employment as electrode materials in MFC systems.

Polyaniline (PANI), a popular paint commonly used in anti-corrosion fields, belongs to a small class of polymers capable of transporting electricity.[87] Therefore, the use of PANI in the preparation of MCFs has received substantial attention because of their high intrinsic electronic and ionic conductivities.[87,88] For example, three chemicals, PANI, iron, and resin-derived carbons containing *in situ* nitrogen (NC) were synthesized to obtain PANI@Fe/NC catalysts (Fig. 9a and b). The products achieved a high power output of 637.53 mW m^{-2}, approximately 36.25% higher than conventional Pt/C cells with 467.92 mW m^{-2}.[87] (Fig. 9c). In addition, the COD removal efficiency of PANI was good, and the overall COD removal by PANI@Fe/NC after 30 days was 84.37% (Fig. 9d). Zhao *et al.*, found that substituting reduced graphene oxide for the Fe/NC electrode led to an increase in maximum power density to 862 mW m^{-2} (1943.71 mA m^{-2} of the current density).[88] In their work, the presence of PANI increased the surface roughness and potential of carbon fibers, thereby promoting the electrogenic performance of

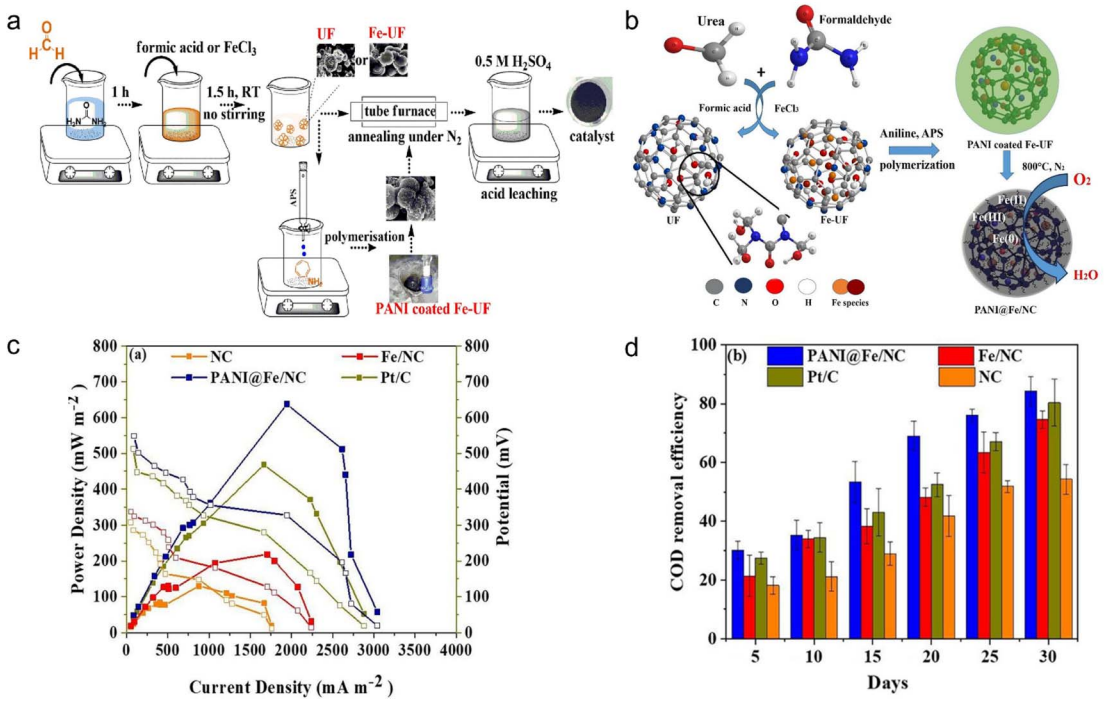

Fig. 9 Preparation of microbial fuel cells using plastic-based MOF materials. (a) PANI@Fe/NC schematic representation of the catalyst synthesis route; (b) schematic representation for the PANI@Fe/NC catalyst; (c) different catalyst polarisation and power density curves (NC, PANI@Fe/NC, Fe/NC, Pt/C); (d) COD removal efficiency from the catalyst-modified MFC systems. The figure has been reproduced from ref. 87 with permission from Elsevier Science, copyright 2022.

MFCs. To be more environmentally friendly, the TA monomer generated from PET plastics was used as the linking unit to synthesize Fe-based MOFs, which were then modified with PANI to form the final MFC electrodes (Fe-TA-MOF/PANI). The MFC has a power density of 680 mW m^{-2} and a limiting current density of 3500 mA m^{-2}.[26] Despite a modest loss in power density, the study provided a promising modifying method for producing high-performance anodes from simple, sustainable and environment-friendly materials in order to achieve bio-energy. Another study created novel MFCs using MOFs and sulfonate polysulfone (SPSU/MIL-100(Fe)). In this study, the SPSU/MIL-100(Fe) operated as a proton-exchange polymer electrolyte and achieved a power density of 27.60 mW m^{-2} and a current density of around 172.67 mA m^{-2}.[83] The systems successfully reduced chemical oxygen demand by around 57.65%. Therefore, this is a novel approach to incorporate polymer-based MOF materials into practical wastewater treatment applications.

The in-plane delocalized π–d conjugation induces superior conductivity in the two-dimensional (2D) MOF materials. Conjugation is mostly achieved by combining conjugated ligand frontier orbitals with transition metal d-orbitals.[89,90] To optimize the transport behaviors of redox electrons and electrolyte ions, a 3D architecture with interpenetrating conductive qualities was devised and synthesized. The poly(3,4-ethylenedioxythiophene) (PEDOT) was coated on MIL-53(Al), synthesized from $Al[NO_3]_3 \cdot H_2O$ and PET-derived TA, *via* simply stirring a combination of EDOT monomer, ammonium peroxodisulphate, and MIL-53(Al) at 900 rpm for 20 h. The precipitate was removed and rinsed with ethanol, and then sonicated for 1 h with a solution of 1 mL isopropyl alcohol and 35 μL Nafion. The 3D cathodes exhibited a four-electron transfer pathway and a power density of 4.78 W m^{-3}, with a cost that ~6.7 times lower than commercial Pt/C cells.[91] Aside from being used directly to construct a 3D structured cathode, the polymer could also be coated on 3D structured MOF materials to avoid water leakage. A typical example involves creating a 2D catecholate-based MOF (M-CAT) and then expanding to 3D structures by coupling with multi-component catalysts (*e.g.*, carbon nanotubes (CNTs)).[89] After constructing the high performance MOF@CNTs nanocomposites, electrostatic spinning technology is used to manufacture PVDF membranes as a gas diffusion layer and collector layer. The PVDF possessed a high resistance to 10 cm height water pressure within 30 days. The CNT-based MOF@PVDF nanocomposites showed higher oxygen permeability (~5.8 mg L^{-1}) compared to the control group (2.2 mg L^{-1}). Higher oxygen permeability resulted in a smooth reaction and a low cost of electricity. Under the conditions, the MFC using CNTs-based NiCO-CAT/PVDF obtained the maximum power density of 530 ± 9 mW m^{-2}, greatly exceeding that of the commercial Pt/C cathode. This work developed unique cathodes for the cost-effective preparation of MFCs and provided new perspectives for improving MFC performance using ORR conductive MOF catalysts.

In the field of plastic-derived MFC technology, the analyzed search results revealed substantial insights into the function of

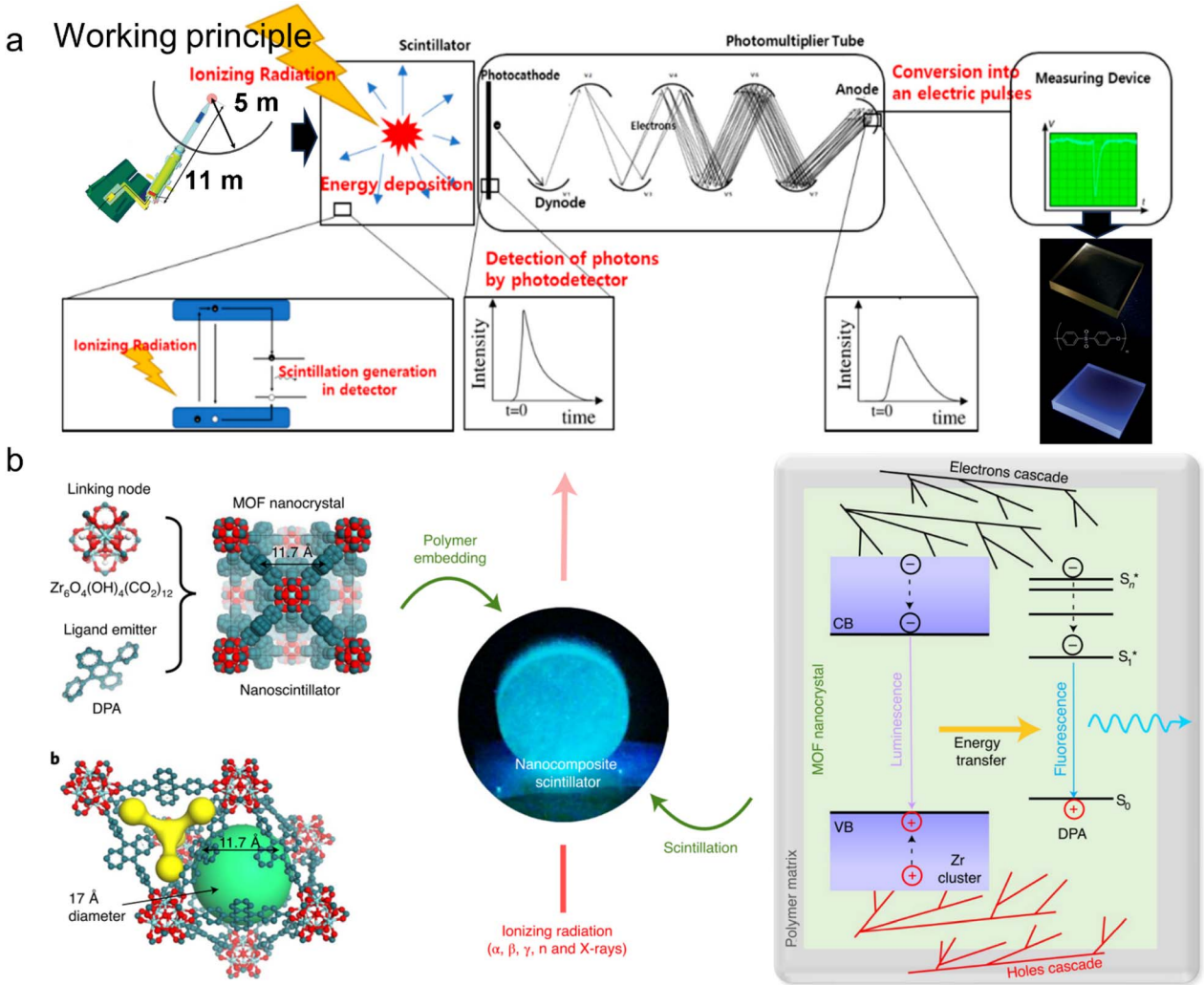

Fig. 10 Plastic scintillators made of MOF@plastic composites. (a) Working principles could be generally summarized as four steps: ionizing radiation interaction, molecule excitation, photon emission/detection, and signal processing. The figure has been reproduced from ref. 91 and 94 with permission from John Wiley and Sons and MDPI, copyright 2022 and 2021; (b) composite plastic scintillator based on fluorescent MOF nanocrystals, including the molecular structure, sketch of the MOF tetrahedral and octahedral cavities, picture of the composite scintillator, and outline of the photophysics involved in the scintillation process. The figure has been reproduced from ref. 79 with permission from Springer Nature, copyright 2016.

plastics with various sorts. The research investigated the integration of plastic-based MOFs into MFC preparation and highlighted the importance of polymers. In terms of sustainable energy development, plastic-based MOFs have to provide synergistic solutions for MFC preparation. The use of such polymer-derived MFCs could provide a novel approach for electrode material discovery, potentially improving electrochemical properties while supporting sustainable development. However, in order to provide comprehensive abstracts on the subject, more in-depth research into the role of plastic-derived MOFs in MFCs should be a requisite.

6.4 Plastic scintillators

Plastic scintillators are fluorescent materials embedded in polymers that emit light when subjected to ionizing radiation.[92] The working principles could be generally summarized as four steps: ionizing radiation interaction, molecule excitation, photon emission/detection, and signal processing (Fig. 10a). Plastic scintillators first absorb the energy from external ionizing radiation (*e.g.,* gamma rays, charged particles), and then promote the molecules within the plastic scintillator to higher energy states. These excited molecules are generally unstable and quickly return to lower but relatively more stable states, releasing excess energy in the form of photons. Photodetectors convert emitted photons to electrical signals, which are then detected and measured based on the intensity and timing of the light pulses. The whole procedures allow plastic scintillators to be sensitive to radioluminescence spectra.[93,94]

MOFs have gradually gained recognition as attractive candidates for the construction of plastic scintillators.[71] Their ligands are adaptable and can be changed, whereas the metal ions allow for increased interaction efficiency of ionizing

radiation (Fig. 10b).[95] Previous studies revealed various common metal ions of Zn^{2+}, Pb^{2+}, Ba^{2+}, or Zr^{4+}-based scintillating coordination polymers, with Zr-based polymers exhibiting superior absorption and emission properties in radioluminescence measurements.[70,71] Prototype scintillators were fabricated by embedding Zr-MOF nanocrystals in polydimethylsiloxane (PDMS) and polymethyl methacrylate (PMMA) polymers under solvothermal conditions at 120 °C for 22 h. After washing and activating at 140 °C, the resultant products exhibited superior radiation hardness (~10% decrease in the RL intensity) and rapid scintillation activation dynamic (<100 ps threshold).[71] On the basis of that, the author used similar self-assembly methods to investigate Zr-MOF@PDMS scintillators with a substantial Stokes shift (750 meV).[70] Such a wide shift allows for excellent contrast images with reduced excitation stray light, thereby saving cost on filtering components and time for image post-processing.[96] These studies open up new possibilities for fabricating highly efficient and sensitive plastic scintillators to enable future photonic and photochemical applications.

In addition to Zr-based MOF@polymer scintillators, lanthanide (Ln) bearing polymers not only can increase luminescence yield but also improve radioluminescence attenuation efficiency due to their heavier metal nature.[97,98] Meanwhile, lanthanides are well-known for their sharp emission,[99] substantial Stokes shift,[100] and several infrared emissions.[101] Therefore, a study confirmed the efficiency and stability of nearly all Ln ions.[102] In their study, the proposed lanthanide complexes were added to styrene (PS monomer) and curing agents before being fully degassed using multiple freeze–pump–thaw cycles in a nitrogen atmosphere. The resultant mixtures were heated, sealed, and placed in an oven at 50 °C for 30 days. Lastly, the items were shaped and polished for further determination. The results showed that the majority of Ln-based MOF@polymers, particularly the Europium (Eu)-based plastic scintillators, were sensitive to low-energy gamma rays. A simulation was carried out to confirm the susceptibility of these plastic scintillators to gamma ray total absorption. This work provided guidance for the design and fabrication of PS scintillators with Eu(III) ion coordination.[102] Although PS presented several advantages in the plastic scintillators like cheap, sensitive, and can be prepared in large volumes, there were some drawbacks that limited chemical development, including poor resolution, time consuming, and relatively low scintillation yields.[92] Several organizations discovered novel polymers for the construction of plastic scintillators.[102–104] PMMA and PMDS are another two representative polymers with more flexible structure, higher near-ultraviolet transparency, and higher scintillation efficiency.[93,98,102–104] Zhang *et al.* synthesized Eu^{3+} and Terbium^{3+} (Tb^{3+}) based MOF@PDMS materials by hydrothermal methods (50–90 °C in a water bath for 12 h).[103] Tb^{3+} ions trap electrons more efficiently than Eu^{3+} due to their vacant 4f orbitals, leading to increased radioluminescence intensity through electron–hole recombination. Another study developed a novel Eu-MOF@polymer scintillator that successfully demonstrated luminescent behavior under ultraviolet light (broadband luminescence from 588–690 nm) and X-ray excitations (2.37–94.7 $m_{Gy_{air}}\ s^{-1}$).[93] Ou *et al.* synthesized nanosized Tb-MOF@polymer scintillators by a co-precipitation method. These scintillators enable X-ray luminescence extension imaging with extended optical memory (>15 days) and high resolution (>20 line pairs mm^{-1}).[98]

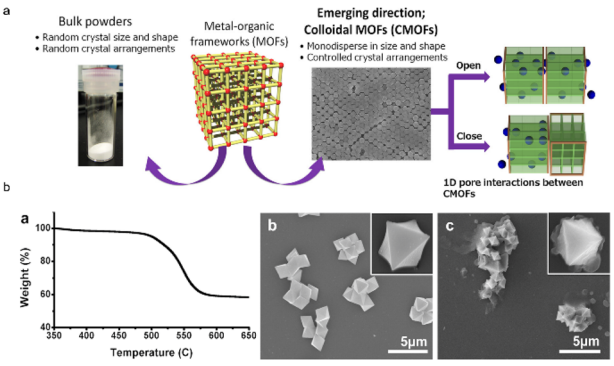

Fig. 11 Sensors made of MOF@plastic materials. (a) CMOFs use particles that are regulated in size and shape instead of bulk powders; (b) thermal gravimetric analysis of colloidal UiO-66 in the laboratory indicates that the 2 μm particles have comparable thermal stability to their bulk counterpart; SEM images show that the particle morphology was retained after heating at 400 °C for 3 h, whereas amorphous carbon formed around the microcrystals, and 600 °C for 3 h. The figure has been reproduced from ref. 107 with permission from American Chemical Society, copyright 2014.

Apart from single metal-based MOFs@plastic products, plastic scintillators use a variety of di-metals and polymers. For example, because both Hf- and Zr-MOFs efficiently convert X-rays into visible light, combining two metals with similar properties can result in improved performance.[105] Since then, many studies have prepared two or more metal-based MOFs involving various polymers, such as $CsPbCl_2Br$@UiO-67-bpy and $CsPbCl_2Br$@MIL-101(Cr).[104] Meanwhile, the polymers in MOF were selected as TA (derived from PET plastics) for MIL-101(Cr) and PS powder for curing and preparation of scintillators. The results showed that all of the samples exhibited broad absorption ranges of photoluminescence from 360–484 nm and a transient lifespan of 2.16–3.25 ns, indicating that the combination of metals might assure improved performance for preparing plastic scintillators.[104] However, related studies are still in their infancy, and further investigations on plastic scintillators are of great urgency in order to reduce costs, speed up response rate and improve performance.

6.5 Sensors

MOFs have been tremendously applied in the construction of sensors.[36] The interconnecting nanochannels created during the manufacture of MOFs play a vital role in the selective transportation of desired ions or fast responses to the variation of external environments (*e.g.,* ionizing radiation and target concentration difference).[106] With polymers as the optimal substrate for incorporation, MOF@plastic composites have improved transport properties and excellent broad surface areas for sensing (Fig. 11a).[107] For example, the fluorescence features of Ln- and Zr–based scintillators could be further applied in

multifunctional luminescent sensors.[72,108–111] Liang *et al.* synthesized nine novel Ln-coordination MOFs with TA through hydrothermal procedures (180 °C for 72 h), and investigated their luminescence properties and thermal stabilities.[108] The results displayed that practically all the Ln-based MOFs had emission bands ranging from 473 to 480 nm. The comparable bands of Eu-MOFs ranged from 579 to 696 nm, while those of Tb-MOFs ranged from 490 to 618 nm. Eu-, Tb-, and Gd-based MOFs showed remarkable sensitivity to Fe^{3+} ions, with limits of detection (LOD) of 4.36×10^{-3} M, 4.18×10^{-3} M, and 4.18×10^{-3} M, respectively. Moreover, the authors found that both the Tb- and Gd-based MOFs could be applied in pH sensing, with the PXRD patterns shifting when the pH value exceeded 7.[108] Since then, several studies have begun to use these kinds of compounds to detect the quantities of cations, pollutant types and environmental parameters (*e.g.,* pH and temperatures).

For heavy metal ions and organic pollutants, Zhou *et al.* developed Eu-based MOFs in a Teflon-lined autoclave at 160 °C for 72 h. They subsequently prepared nano-Eu-MOF@polyacrylonitrile (PAN) using electrospinning technology.[109] The LOD decreased to 6.3×10^{-5} M, indicating enhanced sensing character. Because most heavy metal ions cannot be absorbed and hence disrupt DNA structure, their detections were required to be expanded. Five Ln-based MOFs were designed by immobilizing them in polyvinyl alcohol (PVA) solution.[112] The Eu-/Tb-based MOF can detect not only Fe^{3+} (LOD: 1.17×10^{-3} M and 1.31×10^{-3} M, respectively) but also $Cr_2O_7^{2-}$ (LOD: 8.8×10^{-4} M and 6.8×10^{-4} M, respectively) and CrO_4^{2-} (LOD: 8.1×10^{-4} M and 8.3×10^{-4} M, respectively). Meanwhile, the sensing ability for organic compounds by Ln- and Zr-based MOFs was also developed.[72,113,114] The Tb-MOF was produced and coated on a polylactic acid film, which was then fabricated as a sensor to swiftly identify and quantify phenylglyoxylic acid (PGA), a typical biomarker after exposure to styrene, a carcinogenic substance to humans (category 2B). The sensor detects PGA in urine with high efficiency (LOD: 1.05×10^{-4} mg mL^{-1}) and rapid reaction (less than 10 s). Qu *et al.* fabricated Tb-based MOFs to simultaneously determine dimetridazole, metronidazole and tetracycline hydrate in aqueous, with the LOD of 41.90, 86.48 and 20.30 mg L^{-1}.[114] Meanwhile, Zr-based MOF@PVDF membranes were developed to detect the contents of personal care products (PCPs). Zr-based MOF@PVDF composites have a low LOD of 0.03 μg L^{-1}, promising for detection of parabens and benzophenones. Another study constructed Zr-based MOFs from $ZrCl_4$ and TA in dimethylformamide (DMF) solutions at 120 °C for 24 h.[115] The results illustrated that the system had a detection limit of 1.84×10^{-4} mmol L^{-1} for BPS in commercial plastic bottled water. Therefore, the advancements in Ln- and Zr-MOFs@plastic composites for detecting cations and pollutants are remarkable. The related products could significantly lower the LOD, increase the sensing capabilities, and enhance the response times. Therefore, these studies showcase the innovative potential of MOF@polymer composites in detection of heavy metal ions and organic pollutants.

For common environmental parameters like pH and temperature, an Eu-based MOF@polymer composite was constructed by heating a mixture of Eu-MOF, TA-NH_2 and other solutions (*e.g.,* HCl and DMF) at 120 °C for 24 h.[116] The pH sensitivity of the resulting probe was significantly increased with values ranging from 1.19 to 13.98. The composites exhibited three luminescent response modes: red emission quenching ($1.19 < pH < 7.56$), red emission quenching while blue emission enhancing ($8.36 < pH < 12.04$), and blue emission quenching ($12.20 < pH < 13.98$). In the thermometer, a series of Ln-based MOFs were successfully produced by applying basic covalent crosslinking methods (100 °C for 4 h), then were coated onto polyimide (PI) and polytetrafluoroethylene (PTFE) substrates by heating in an oven at 120 °C for 2 h.[110] Under these conditions, the MOF@plastic composites operate over a wide temperature range (77–297 K at 390 nm; 273–393 K at 454 nm).[110] Similarly, another study used Tb^{3+}-Eu^{3+}-based Ln-MOFs as thermometers to reflect temperatures ranging from 80 to 280 K.[117] The findings were anticipated to shed fresh light on the application of Ln-based MOFs in temperature sensing when paired with other polymer matrix materials. In particular, UiO-66 showed good thermal stability in Zr-MOF, and the results showed that the particle morphology of colloidal UiO-66 was almost unchanged at 600 °C (Fig. 11b). These MOF@polymer composites revealed intriguing uses in environmental sensing fields. Their applications could result in considerable enhancements in pH and temperature sensitivity, which is critical for precise environmental monitoring. The advancements demonstrate the promise of MOFs in developing more efficient and sensitive environmental sensors.

In addition to the Zr- and Ln-based MOFs, other common metal-based MOF@polymer composites were also applied to sense the concentration of contaminants.[111,118–122] Wang *et al.* used hydrothermal processes to develop Cu-MOF from copper nitrate trihydrate, TA, and triethylenediamine in DMF solutions. The LOD of BPA was 13 nmol L^{-1}, much lower than in Zr-based MOFs.[119] The result suggested that common metal-based MOF biosensors could be a promising candidate for ultrasensitive bisphenol detection. Except for Cu, other common metals like Zn also displayed great sensitivities on other contaminants, with the LOD as low as for methane (ZIF-8 MOFs@PDMS), 0.28 μM for PGA (Zn-MOFs@TA), and 0.333 μM for glucose (ZIF-8 MOFs@polydopamine) in real samples. However, the related studies are still in their early stages, and the sensing mechanism is largely unclear. Therefore, increasing the physicochemical characterization is of urgent necessity to reveal the sensing interactions of MOF@plastic composites in real-world environments or human samples.

7. Conclusions and outlook

The extensive use of plastics without adequate control management will result in huge generations of microplastics, ultimately posing threats to the environment and human health. Recent studies have focused on extensive treatments of environmental MPs, among which MOF materials exhibited promising potential in the adsorption, degradation, and composition of MPs/plastics due to their tunable structures, high specific surface area, accessible active sites and superior

composite properties. Therefore, we explored the adsorption capabilities of MOFs for MPs/plastics in aquatic environments, the efficiencies of MPs/plastics catalyzed by MOF materials, and the multifunctional applications of MOF@plastic composites.

Many MOF materials displayed prominent efficiencies (>90%) for removing MPs/plastic particles *via* hydrophobic interaction, electrostatic attraction, π–π stacking, and van der Waals forces. However, most recent studies mainly examined adsorption in simulated environments, like the presence of only target ions in the Milli-Q water (Challenge 1). Future studies should be concentrated on more complex environments, including real water samples. Meanwhile, the interaction mechanisms between MPs/plastic particles and MOF materials should be turned on the agenda, which could be revealed by conducting experiments on adsorption kinetics, isotherms and thermodynamics (Prospect 1).

Several Zr- or Ln-based MOF materials can successfully convert various types of plastics (*e.g.*, PE, PET, PEG, and poly(g-butyrolactone)) into harmless molecules, including MMT and TA, as well as high-valued substances like H_2 or CH_4. The degradation mechanisms obtained in these studies are diverse. In thermocatalysis, the C–O bonds in MPs/plastics could be broken at higher temperatures, resulting in carboxylic acid-terminated units through hydrogenolysis. With a continuous thermolysis process, MMT and TA should be generated. The procedures necessitated a heat treatment, which might consume the heat energy. Therefore, how to decrease energy consumption should be the next challenge (Challenge 2). In photocatalysis, ROS could interact with oxygen to generate ROO· or ROOH. ROOH could further generate ROO· and ·OH groups through chain propagation reactions. However, their detailed catalytic mechanisms remain limited, with unexplainable byproducts generated (Challenge 3). Therefore, more efforts are urged to understand the generation of intermediate products and the degradation path of photocatalytic conversion of plastics by novel technologies (*e.g.,* mass spectrometry) (Prospect 2), as well as to benefit from verification simulations (*e.g.,* density functional theory calculations) (Prospect 3). Moreover, MPs/plastics degradation is still in its infancy, with some being successfully converted into harmless or even highly-valued substances (*e.g.*, PE, PET, PEG, and poly(g-butyrolactone)), but little research has been reported on the degradation of other types of aged MPs/plastics (*e.g.,* PVC) due to the generation of side reactions and toxic gases (*e.g.,* Cl_2) (Challenge 4). Therefore, investigations are necessary for creating more advanced degrading techniques for various types of MPs/plastics, which might be helpful in a wide range of industrial applications (Prospect 4).

Because of the polymer's endurance, strength, and cost-effectiveness, many studies have paid attention to employing MPs/plastics as ligands to construct MOF materials through three dominant ways: glycolysis, hydrolysis and methanolysis. The three ways involve the fragmentation of long polymer chains of the MPs/plastics at high temperatures and pressures with several advantages of environmentally friendliness, high quality and excellent purity of the products. However, the disadvantages of energy and time consumption are also evident throughout the preparation processes (Challenge 5). Future analysis should focus on how to conduct the procedure more economically while improving conversion efficiency (Prospect 5).

Finally, the multifunctional applications of MOF@plastic composites were discussed from the following aspects, especially in sewage treatment, gas adsorption/separation, and preparations of MFCs, plastic scintillators and other sensors. In sewage treatment, waste plastic-derived MOFs demonstrated high heavy metals and organic pollutant removal efficiencies even after multiple adsorption cycles. They demonstrated remarkable efficiency for gradient gas adsorption with similar concepts. However, most of the present articles focused on MOF@plastic composites only derived from waste PET (Challenge 6), developing other types of plastics applied for MOF preparation should be considered in further studies (Prospect 6). In device preparation, plastic-derived MOF materials demonstrated superior electrical catalytic oxidation–reduction reactions. Nevertheless, a major impediment to the direct use of polymers as nodes is the limited availability of conducting polymers (Zr- and Ln- MOFs) (Challenge 7), which need more development in preparing MFCs using various polymer-based MOFs as sustainable anodes or cathodes for catalytic application in air cathodes (Prospect 7). Although several different metals were utilized in preparing plastic scintillators with outstanding optical memory and high resolution, more investigations on plastic scintillators are urgently needed to create novel plastic scintillators with less costs and faster responses (Prospect 8). Meanwhile, these publications were mainly engrossed in pristine polymers, improved scintillators derived from waste plastics should be another great challenge (Challenge 8). The review finally summarized that MOF@plastic composite materials had excellent sensing abilities in detecting cations, contaminants and environment conditions at extremely low LODs of ppm or even the ppt level. However, two critical challenges emerged regarding the sensing method and the unavailability of real environmental or human samples (Challenge 9). More advanced physicochemical characterization studies are required to reveal the sensing interactions of MOF@plastic composites in real environmental or human samples (Prospect 9). The review can better understand the relationships between MPs/plastics and MOF materials, providing a deeper insight into how MOFs remove and degrade MP/plastic particles, as well as how MPs/plastics can be recycled to prepare MOFs. Overall, this review is anticipated to outline future directions for turning the threats (MPs/plastics contamination) into opportunities (*e.g.,* as ligands for MOF or MOF@-plastic materials for further applications).

Data availability

Data sharing is not applicable to this article as no datasets were generated or analysed during the current study.

Author contributions

Pengfei Wu: conceptualization, funding acquisition, methodology, writing – original draft, writing – review & editing.

Mengting Guo: data curation, investigation, methodology, writing. Guibin Wang: data curation, formal analysis, investigation. Qing Huang: conceptualization, formal analysis, funding acquisition, methodology, supervision, writing – original draft, writing – review & editing. Yaqian Lan: conceptualization, funding acquisition, methodology, supervision.

Conflicts of interest

The authors declare they have no conflicts of interest.

Acknowledgements

This work was supported financially by the National Natural Science Foundation of China (NSFC: 22106130, 22101089, 22471126, and 22225109) and Jiangsu Specially-Appointed Professor Program.

Notes and references

1 A. D. Vethaak and J. Legler, *Science*, 2021, **371**, 672–674.
2 Statista, Annual production of plastics worldwide from 1950 to 2022, **https://www.statista.com/statistics/282732/global-production-of-plastics-since-1950/**, (accessed June 2024).
3 A. Isobe, S. Iwasaki, K. Uchida and T. Tokai, *Nat. Commun.*, 2019, **10**, 1–3.
4 K. R. Vanapalli, H. B. Sharma, V. P. Ranjan, B. Samal, J. Bhattacharya, B. K. Dubey and S. Goel, *Sci. Total Environ.*, 2021, **750**, 141514.
5 R. Geyer, J. R. Jambeck and K. L. Law, *Sci. Adv.*, 2017, **3**, 25–29.
6 P. Wu, H. Zhang, N. Singh, Y. Tang and Z. Cai, *Chem. Eng. J.*, 2022, **429**, 132351.
7 S. Lin, H. Zhang, C. Wang, X. Su, Y. Song, P. Wu, Z. Yang, M. Wong, Z. Cai and C. Zheng, *Environ. Sci. Technol.*, 2022, **56**, 12483–12493.
8 Y. Jin, L. Lu, W. Tu, T. Luo and Z. Fu, *Sci. Total Environ.*, 2019, **649**, 308–317.
9 L. Lu, Z. Wan, T. Luo, Z. Fu and Y. Jin, *Sci. Total Environ.*, 2018, **631–632**, 449–458.
10 A. T. B. Guimaraes, I. Charlie-Silva and G. Malafaia, *J. Hazard. Mater.*, 2021, **407**, 124833.
11 C. Lee, L. Hsu, I. Wu, Y. Wang, W. Chen, Y. Liu, L. Yang, C. Tan, Y. Luo, C. Wang, H. Chiu, T. C. Yang, Y. Lin, H. Chang, Y. Chiang, C. Chen, M. Lee, K. Peng and C. Chia, *J. Hazard. Mater.*, 2022, **430**, 128431.
12 A. D. Gray and J. E. Weinstein, *Environ. Toxicol. Chem.*, 2017, **36**, 3074–3080.
13 P. Wu, S. Lin, G. Cao, J. Wu, H. Jin and C. Wang, *J. Hazard. Mater.*, 2022, **437**, 129361.
14 J. Chen, J. Wu, P. C. Sherrell, J. Chen, H. Wang, W. xian Zhang and J. Yang, *Adv. Sci.*, 2022, **9**, 1–36.
15 E. D. Okoffo, F. Ribeiro, J. W. O'Brien, S. O'Brien, B. J. Tscharke, M. Gallen, S. Samanipour, J. F. Mueller and K. V. Thomas, *Sci. Total Environ.*, 2020, **715**, 136924.
16 P. Wu, B. Wang, Y. Lu, G. Cao, P. Xie, W. Wang, D. Chen, G. Huang, H. Jin, Z. Yang and Z. Cai, *ACS EST Water*, 2024, **4**, 1107–1118.
17 M. Wagner and S. Lambert, *Freshwater Microplastics: Emerging Environmental Contaminants?*, Springer, Heidelberg, 2018, p. 302.
18 X. Jie, W. Li, D. Slocombe, Y. Gao, I. Banerjee, S. Gonzalez-cortes, B. Yao, H. Almegren, S. Alshihri, J. Dilworth, J. Thomas, T. Xiao and P. Edwards, *Nat. Catal.*, 2024, **4**, 1107–1118.
19 X. Jiao, K. Zheng, Q. Chen, X. Li, Y. Li, W. Shao, J. Xu, J. Zhu, Y. Pan, Y. Sun and Y. Xie, *Angew. Chem., Int. Ed.*, 2020, **59**, 15497–15501.
20 J. He, L. Han, F. Wang, C. Ma, Y. Cai, W. Ma, E. G. Xu, B. Xing and Z. Yang, *Crit. Rev. Environ. Sci. Technol.*, 2022, 1–23.
21 Z. Zhang, H. Peng, D. Yang, G. Zhang, J. Zhang and F. Ju, *Nat. Commun.*, 2022, **13**, 5360.
22 J. M. Garcia and M. L. Robertson, *Science*, 2017, **358**, 870–872.
23 Y. Chen, Y. Chen, Y. Chen, Y. Chen, Y. Qi, H. Zhu, X. Huang and Y. Wang, *Chem*, 2021, **7**, 1–17.
24 X. Jiao, K. Zheng, Q. Chen, X. Li, Y. Li, W. Shao, J. Xu, J. Zhu, Y. Pan, Y. Sun and Y. Xie, *Angew. Chem.*, 2020, **132**, 15627–15631.
25 R. Kaur, A. Marwaha, V. A. Chhabra, K. Kaushal, K. H. Kim and S. K. Tripathi, *J. Cleaner Prod.*, 2020, **263**, 121492.
26 R. Kaur, S. Singh, V. A. Chhabra, A. Marwaha, K. H. Kim and S. K. Tripathi, *J. Hazard. Mater.*, 2021, **417**, 125992.
27 B. Slater, S. O. Wong, A. Duckworth, A. J. P. White, M. R. Hill and B. P. Ladewig, *Chem. Commun.*, 2019, **55**, 7319–7322.
28 Y. Wang, H. Wang, S. Li and S. Sun, *ACS Omega*, 2022, **7**, 35180–35190.
29 W. J. Koros and C. Zhang, *Nat. Mater.*, 2017, **16**, 289–297.
30 P. Kalimuthu, Y. Kim, M. P. Subbaiah, D. Kim, B. H. Jeon and J. Jung, *Chemosphere*, 2022, **294**, 133672.
31 Q. Huang, T. Wei, M. Zhang, L. Z. Dong, A. M. Zhang, S. L. Li, W. J. Liu, J. Liu and Y. Q. Lan, *J. Mater. Chem. A*, 2017, **5**, 8477–8483.
32 Y. R. Wang, Q. Huang, C. T. He, Y. Chen, J. Liu, F. C. Shen and Y. Q. Lan, *Nat. Commun.*, 2018, **9**, 1–8.
33 Q. Huang, Q. Niu, X. Li, J. Liu, S. Sun, L. Dong, S. Li, Y. Cai and Y. Lan, *Sci. Adv.*, 2022, **8**, eadd5598.
34 D. Panda, S. Patra, M. K. Awasthi and S. K. Singh, *J. Chem. Educ.*, 2020, **97**, 1101–1108.
35 R. B. Lin, S. Xiang, W. Zhou and B. Chen, *Chem*, 2020, **6**, 337–363.
36 G. W. Peterson, D. T. Lee, H. F. Barton, T. H. Epps and G. N. Parsons, *Nat. Rev. Mater.*, 2021, **6**, 605–621.
37 T. F. Mastropietro, *Sci. Technol. Adv. Mater.*, 2023, **24**, 2189890.
38 P. Wu, Z. Cai, H. Jin and Y. Tang, *Sci. Total Environ.*, 2019, **650**, 671–678.
39 F. Pasanen, R. O. Fuller and F. Maya, *Chem. Eng. J.*, 2022, **455**, 140405.
40 D. You, Y. Zhao, W. Yang, Q. Pan and J. Li, *Chem. Res. Chin. Univ.*, 2022, **38**, 186–191.

41 M. Haris, M. W. Khan, A. Zavabeti, N. Mahmood and N. Eshtiaghi, *Chem. Eng. J.*, 2023, **455**, 140390.
42 A. A. Mohana, M. Rahman, S. K. Sarker, N. Haque, L. Gao and B. K. Pramanik, *Chemosphere*, 2022, **309**, 136682.
43 D. Pedrero, C. Edo, F. Fernández-Piñas, R. Rosal and S. Aguado, *Sep. Purif. Technol.*, 2024, **333**, 125816.
44 M. A. Biamonte and A. Vaselia, *Helv. Chim. Acta*, 1998, **26**, 695.
45 Y. Wu, X. Wang, K. O. Kirlikovali, X. Gong, A. Atilgan, K. Ma, N. M. Schweitzer, N. C. Gianneschi, Z. Li, X. Zhang and O. K. Farha, *Angew. Chem., Int. Ed.*, 2022, **61**, e202117528.
46 Y. Chen, S. Zhang, S. Cao, S. Li, F. Chen, S. Yuan, C. Xu, J. Zhou, X. Feng, X. Ma and B. Wang, *Adv. Mater.*, 2017, **29**, 1606221.
47 Y. Chen, Y. J. Chen, Y. Qi, H. J. Zhu, X. Huang, Y. R. Wang, R. X. Yang, Y. H. Kan, S. L. Li and Y. Q. Lan, *Chem*, 2021, **7**, 463–479.
48 J. Qin, Y. Dou, F. Wu, Y. Yao, H. R. Andersen, C. Hélix-Nielsen, S. Y. Lim and W. Zhang, *Appl. Catal., B*, 2022, **319**, 121940.
49 S. Gazi, M. Đokić, K. F. Chin, P. R. Ng and H. Sen Soo, *Adv. Sci.*, 2019, **6**, 1902020.
50 H. Liu, Y. Feng, J. Shao, Y. Chen, Z. L. Wang, H. Li, X. Chen and Z. Bian, *Nano Energy*, 2020, **70**, 104499.
51 E. S. M. El-Sayed and D. Yuan, *Green Chem.*, 2020, **22**, 4082–4104.
52 K. Boukayouht, L. Bazzi and S. El Hankari, *Coord. Chem. Rev.*, 2023, **478**, 214986.
53 A. S. Goje and S. Mishra, *Macromol. Mater. Eng.*, 2003, **288**, 326–336.
54 D. A. Cabrera-unguia, M. I. León-Campos, J. A. Claudio-Rizo, D. A. Solís-Casados, T. E. Flores-Guia and L. F. Cano Salazar, *Bull. Mater. Sci.*, 2021, **44**, 245.
55 R. X. Yang, Y. T. Bieh, C. H. Chen, C. Y. Hsu, Y. Kato, H. Yamamoto, C. K. Tsung and K. C. W. Wu, *ACS Sustain. Chem. Eng.*, 2021, **9**, 6541–6550.
56 Q. Suo, J. Zi, Z. Bai and S. Qi, *Catal. Lett.*, 2017, **147**, 240–252.
57 V. F. Yusuf, N. I. Malek and S. K. Kailasa, *ACS Omega*, 2022, **7**, 44507–44531.
58 M. Pander, M. Janeta and W. Bury, *ACS Appl. Mater. Interfaces*, 2021, **13**, 8344–8352.
59 Z. Liu and Y. Liu, *ACS Symp. Ser.*, 2021, **1394**, 1–31.
60 L. Biermann, E. Brepohl, C. Eichert, M. Paschetag, M. Watts and S. Scholl, *Green Process. Synth.*, 2021, **10**, 361–373.
61 L. D. Ellis, N. A. Rorrer, K. P. Sullivan, M. Otto, J. E. McGeehan, Y. Román-Leshkov, N. Wierckx and G. T. Beckham, *Nat. Catal.*, 2021, **4**, 539–556.
62 W. Yang, R. Liu, C. Li, Y. Song and C. Hu, *Waste Manage.*, 2021, **135**, 267–274.
63 X. Zhang, K. Yue, R. Rao, J. Chen, Q. Liu, Y. Yang, F. Bi, Y. Wang, J. Xu and N. Liu, *Appl. Catal., B*, 2022, **310**, 121300.
64 A. Sarno, K. Olafsen, S. Kubowicz, F. Karimov, S. T. L. Sait, L. Sørensen and A. M. Booth, *Environ. Sci. Technol. Lett.*, 2021, **8**, 250–255.
65 Y. Zhu, L. Ouyang, H. Zhong, J. Liu, H. Wang, H. Shao, Z. Huang and M. Zhu, *Angew. Chem.*, 2020, **132**, 8701–8707.
66 A. U. R. Bacha, I. Nabi, M. Zaheer, W. Jin and L. Yang, *Sci. Total Environ.*, 2023, **858**, 160108.
67 D. D. Pham and J. Cho, *Green Chem.*, 2021, **23**, 511–525.
68 M. Genta, T. Iwaya, M. Sasaki, M. Goto and T. Hirose, *Ind. Eng. Chem. Res.*, 2005, **44**, 3894–3900.
69 B. V. K. J. Schmidt, *Macromol. Rapid Commun.*, 2020, **41**, 1900333.
70 J. Perego, C. X. Bezuidenhout, I. Villa, F. Cova, R. Crapanzano, I. Frank, F. Pagano, N. Kratochwill, E. Auffray, S. Bracco, A. Vedda, C. Dujardin, P. E. Sozzani, F. Meinardi, A. Comotti and A. Monguzzi, *Nat. Commun.*, 2022, **13**, 1–10.
71 J. Perego, I. Villa, A. Pedrini, E. C. Padovani, R. Crapanzano, A. Vedda, C. Dujardin, C. X. Bezuidenhout, S. Bracco, P. E. Sozzani, A. Comotti, L. Gironi, M. Beretta, M. Salomoni, N. Kratochwil, S. Gundacker, E. Auffray, F. Meinardi and A. Monguzzi, *Nat. Photonics*, 2021, **15**, 393–400.
72 P. Jia, L. Gao, Y. Zheng, X. Zheng, C. Wang, C. Yang, Y. Li and Y. Zhao, *ACS Appl. Mater. Interfaces*, 2021, **13**, 33546–33556.
73 S. Singh, S. Sharma, A. Umar, M. Jha, S. K. Mehta and S. K. Kansal, *New J. Chem.*, 2018, **42**, 1921–1930.
74 V. D. Doan, T. L. Do, T. M. T. Ho, V. T. Le and H. T. Nguyen, *Sep. Sci. Technol.*, 2020, **55**, 444–455.
75 J. Hu, Y. Wang and L. Wu, *J. Phys.: Conf. Ser.*, 2022, **2194**, 012005.
76 D. S. Sholl and R. P. Lively, *Nature*, 2016, **532**, 435–437.
77 X. Dyosiba, J. Ren, N. M. Musyoka, H. W. Langmi, M. Mathe and M. S. Onyango, *Sustainable Mater. Technol.*, 2016, **10**, 10–13.
78 X. Dyosiba, J. Ren, N. M. Musyoka, H. W. Langmi, M. Mathe and M. S. Onyango, *Ind. Eng. Chem. Res.*, 2019, **58**, 17010–17016.
79 J. Ren, X. Dyosiba, N. M. Musyoka, H. W. Langmi, B. C. North, M. Mathe and M. S. Onyango, *Int. J. Hydrogen Energy*, 2016, **41**, 18141–18146.
80 J. Ren, N. M. Musyoka, H. W. Langmi, B. C. North, M. Mathe, X. Kang and S. Liao, *Int. J. Hydrogen Energy*, 2015, **40**, 10542–10546.
81 L. Zhou, S. Wang, Y. Chen and C. Serre, *Microporous Mesoporous Mater.*, 2019, **290**, 109674.
82 X. Jiang, J. Hu, E. R. Petersen, L. A. Fitzgerald, C. S. Jackan, A. M. Lieber, B. R. Ringeisen, C. M. Lieber and J. C. Biffinger, *Nat. Commun.*, 2013, **4**, 2751.
83 B. Roshanravan, H. Younesi, M. Abdollahi, M. Rahimnejad and S. H. Pyo, *J. Cleaner Prod.*, 2021, **300**, 126963.
84 K. P. Katuri, N. M. S. Bettahalli, X. Wang, G. Matar, S. Chisca, S. P. Nunes and P. E. Saikaly, *Adv. Mater.*, 2016, **28**, 9504–9511.
85 Q. Huang, Y. Lan, P. Wu, X. Li, Y. Wang and D. Tian, *Aggregate*, 2024, 1–22.
86 K. Zhong, L. Huang, M. Li, Y. Dai, Y. Wang, J. Zuo, H. Zhang, B. Zhang, S. Yang, J. Tang, J. Yan and M. Su, *Int. J. Hydrogen Energy*, 2019, **44**, 30127–30140.
87 S. K. Dhillon and P. P. Kundu, *Chem. Eng. J.*, 2022, **431**, 133341.

88 N. Zhao, Z. Ma, H. Song, D. Wang and Y. Xie, *Int. J. Hydrogen Energy*, 2018, **43**, 17867–17872.
89 Y. Qin, H. Li, Y. Sun, S. Guo, C. Shi, Y. Liu and C. Li, *J. Power Sources*, 2022, **541**, 231685.
90 D. Xing, Y. Wang, P. Zhou, Y. Liu, Z. Wang, P. Wang, Z. Zheng, H. Cheng, Y. Dai and B. Huang, *Appl. Catal., B*, 2020, **278**, 119295.
91 P. Mukherjee, U. Sharma and P. Saravanan, *Int. J. Energy Res.*, 2022, **46**, 23326–23340.
92 G. H. V. Bertrand, M. Hamel and F. Sguerra, *Chem.–Eur. J.*, 2014, **20**, 15660–15685.
93 W. Zhu, H. Yu, X. Zhu and H. Li, *Inorg. Chem. Commun.*, 2022, **136**, 109182.
94 S. Min, H. Kang, B. Seo, J. Cheong, C. Roh and S. Hong, *Energies*, 2021, **14**, 1–43.
95 F. P. Doty, C. A. Bauer, A. J. Skulan, P. G. Grant and M. D. Allendorf, *Adv. Mater.*, 2009, **21**, 95–101.
96 T. B. Ren, W. Xu, W. Zhang, X. X. Zhang, Z. Y. Wang, Z. Xiang, L. Yuan and X. B. Zhang, *J. Am. Chem. Soc.*, 2018, **140**, 7716–7722.
97 Z. Zeng, B. Huang, X. Wang, L. Lu, Q. Lu, M. Sun, T. Wu, T. Ma, J. Xu, Y. Xu, S. Wang, Y. Du and C. H. Yan, *Adv. Mater.*, 2020, **32**, 1–10.
98 X. Ou, X. Qin, B. Huang, J. Zan, Q. Wu, Z. Hong, L. Xie, H. Bian, Z. Yi, X. Chen, Y. Wu, X. Song, J. Li, Q. Chen, H. Yang and X. Liu, *Nature*, 2021, **590**, 410–415.
99 L. E. MacKenzie and R. Pal, *Nat. Rev. Chem*, 2021, **5**, 109–124.
100 B. Zhou, B. Shi, D. Jin and X. Liu, *Nat. Nanotechnol.*, 2015, **10**, 924–936.
101 Y. Gu, Z. Guo, W. Yuan, M. Kong, Y. Liu, Y. Liu, Y. Gao, W. Feng, F. Wang, J. Zhou, D. Jin and F. Li, *Nat. Photonics*, 2019, **13**, 525–531.
102 G. H. V. Bertrand, M. Hamel, J. Dumazert, R. Coulon and C. Frangville, *Polym. Adv. Technol.*, 2021, **32**, 748–754.
103 X. Zhang, H. Qiu, W. Luo, K. Huang, Y. Chen, J. Zhang, B. Wang, D. Peng, Y. Wang and K. Zheng, *Adv. Sci.*, 2023, **10**, 1–7.
104 C. Ren, Z. Li, L. Huang, X. Xiong, Z. Nie, Y. Yang, W. Zhu, W. Yang and L. Wang, *Nanoscale*, 2022, **14**, 4216–4224.
105 C. Wang, O. Volotskova, K. Lu, M. Ahmad, C. Sun, L. Xing and W. Lin, *J. Am. Chem. Soc.*, 2014, **136**, 6171–6174.
106 Y. Lu, X. Zhang, L. Zhao, H. Liu, M. Yan, X. Zhang, K. Mochizuki and S. Yang, *Nat. Commun.*, 2023, **14**, 1–12.
107 M. Sindoro, N. Yana, A. Y. Jee and S. Granick, *Acc. Chem. Res.*, 2014, **47**, 459–469.
108 Y. Y. Liang, L. L. Xue, H. M. Hu, L. N. Zheng, X. Wang and G. Xue, *J. Solid State Chem.*, 2019, **276**, 6–18.
109 Z. Zhou, M. Shang, Z. Yao and J. Zhang, *Dyes Pigm.*, 2022, **198**, 110016.
110 H. Guan, M. Qi, L. Shi, W. Liu, L. Yang and W. Dou, *ACS Appl. Mater. Interfaces*, 2023, **15**, 18114–18124.
111 R. Cao, H. Ding, K. J. Kim, Z. Peng, J. Wu, J. T. Culp, P. R. Ohodnicki, E. Beckman and K. P. Chen, *Sens. Actuators, B*, 2020, **324**, 128627.
112 S. Wang, B. Sun, Z. Su, G. Hong, X. Li, Y. Liu, Q. Pan and J. Sun, *Inorg. Chem. Front.*, 2022, **9**, 3259–3266.
113 A. Gutiérrez-Serpa, T. Kundu, J. Pasán, A. I. Jiménez-Abizanda, S. Kaskel, I. Senkovska and V. Pino, *ACS Appl. Mater. Interfaces*, 2022, **14**, 4510–4521.
114 Z. Qu, D. Wu, J. Jin, G. Yang and Y. Y. Wang, *J. Solid State Chem.*, 2022, **309**, 123003.
115 C. Liang, Y. Wang, T. Zhang, H. Nie, Y. Han and J. Bai, *Talanta*, 2023, **253**, 123942.
116 W. Ma, X. Quan and B. Yan, *Dyes Pigm.*, 2022, **206**, 110648.
117 T. Liu, S. T. Zhou, S. S. Zhao, H. Zhang, P. Tian and Z. Zhao, *J. Mater. Sci.*, 2023, **58**, 7690–7701.
118 Y. Wang, H. Wang, S. Li and S. Sun, *ACS Omega*, 2022, **7**, 35180–35190.
119 X. Wang, X. Lu, L. Wu and J. Chen, *Biosens. Bioelectron.*, 2015, **65**, 295–301.
120 Y. Chen, X. Sun, S. Biswas, Y. Xie, Y. Wang and X. Hu, *Biosens. Bioelectron.*, 2019, **141**, 111470.
121 D. Song, X. Ji, Y. Li, S. Wu, Y. Zhang, X. Wang, Y. Sun, E. Gao and M. Zhu, *Dalton Trans.*, 2022, **51**, 16266–16273.
122 Y. Wang, C. Hou, Y. Zhang, F. He, M. Liu and X. Li, *J. Mater. Chem. B*, 2016, **4**, 3695–3702.
123 H. Wan, J. Wang, X. Sheng, J. Yan, W. Zhang and Y. Xu, *Toxics*, 2022, **10**, 10020070.
124 S. Modak, M. Kasula and M. R. Esfahani, *ACS Appl. Eng. Mater.*, 2023, **1**, 744–755.
125 Y. J. Chen, Y. Chen, C. Miao, Y. R. Wang, G. K. Gao, R. X. Yang, H. J. Zhu, J. H. Wang, S. L. Li and Y. Q. Lan, *J. Mater. Chem. A*, 2020, **8**, 14644–14652.
126 G. Gnanasekaran, G. Arthanareeswaran and Y. Sun, *Sep. Purif. Technol.*, 2021, **277**, 119655.